

THE UNIVERSITY OF CHICAGO

RADIAL MOTIONS IN SPIRAL GALAXIES

A DISSERTATION SUBMITTED TO
THE FACULTY OF THE DIVISION OF THE PHYSICAL SCIENCES
IN CANDIDACY FOR THE DEGREE OF
DOCTOR OF PHILOSOPHY

DEPARTMENT OF PHYSICS

BY
GREG ROELOFS

CHICAGO, ILLINOIS
DECEMBER 1995

For Dad,
who would have liked to have seen this.

TABLE OF CONTENTS

LIST OF FIGURES	vi
LIST OF TABLES	vii
ACKNOWLEDGMENTS	ix
ABSTRACT	xi
Chapter	
1. INTRODUCTION	1
2. THEORY	5
3. PROCEDURE	12
4. RESULTS	16
4.1 Faked Galaxies	16
4.2 NGC 3198	22
4.3 NGC 6503	30
4.4 NGC 2403	38
4.5 NGC 7331	46
4.6 NGC 2903	54
4.7 NGC 628	62
5. DISCUSSION	72
6. CONCLUSIONS	78
Appendix	
A. SCAN-BASED DATA ANALYSIS	81
REFERENCES	84

LIST OF FIGURES

Figure	Page
1. Velocity Maps for the Six Galaxies	2
2. Faked Velocity Maps	8
3. Faked Planar Galaxy Oscillating in the Fundamental Radial Mode . . .	18
4. Faked Planar Galaxy Oscillating in a Single-Node Radial Mode	20
5. NGC 3198 Radial Fits	24
6. NGC 3198 Residuals	26
7. NGC 3198 Tilted-Rings Fits	28
8. NGC 6503 Tilted-Rings Fits	32
9. NGC 6503 Radial Fits	34
10. NGC 6503 Residuals	36
11. NGC 2403 Tilted-Rings Fits	40
12. NGC 2403 Radial Fits	42
13. NGC 2403 Residuals	44
14. NGC 7331 Residuals	48
15. NGC 7331 Tilted-Rings Fits	50
16. NGC 7331 Radial Fits	52
17. NGC 2903 Tilted-Rings Fits	56
18. NGC 2903 Radial Fits	58
19. NGC 2903 Residuals	60
20. NGC 628 Tilted-Rings Fits	64
21. NGC 628 Residuals	66
22. NGC 628 Radial Fits, Circular Velocity Allowed to Vary	68
23. NGC 628 Radial Fits, Circular Velocity Fixed Beyond 4'	70
24. Faked Velocity Maps at Various Viewing Angles	74

LIST OF TABLES

Table	Page
1. Comparison of Fitting Parameters for the Three Models	13

ACKNOWLEDGMENTS

There are several people who deserve thanks for their support and encouragement during the many years that went into this dissertation, but first and foremost among them is my advisor, Professor Richard H. Miller of the Department of Astronomy and Astrophysics at the University of Chicago. Without his guidance, wit and gentle prodding, I might never have completed this journey.

I also wish to thank my family, both immediate and extended, whose patience and occasional nagging finally had the desired effect. Special thanks are reserved for Veronica for putting up with too many years as the wife of a graduate student, and for my daughter, Lyra, for such a well-timed birth.

Computations were made possible by means of a grant of computing services from the Numerical Aerodynamic Simulation (NAS) Facility at NASA Ames Research Center, which is gratefully acknowledged. In addition, parts of this research were supported by NASA Graduate Student Researchers Program grant NGT-50348. I am most grateful for that support as well.

Finally, I wish to acknowledge the research of K. Begeman; J. Kamphuis and F. Briggs; and R. H. Miller and B. F. Smith. Their work provided the basis for the research presented here.

ABSTRACT

Spiral galaxies are often pictured as stately pinwheels rotating quietly in space, subject to some warping but basically well-behaved. In fact, they exist in a very dynamic environment and are not nearly so simple as they might outwardly appear. There is now strong theoretical evidence to suggest that the massive dark halos that surround spirals oscillate in normal modes (Miller and Smith 1994). If this is so, then a halo's gravitational potential will carry the embedded spiral disk along with it, adding a radial component to velocities that are normally thought of as purely circular. Standard models for disk galaxies do not take this into account. We analyze kinematic data for six galaxies and explicitly look for evidence of large-scale (global) radial flows. We find nothing that rules out such a velocity component, but also nothing that strongly confirms its presence. In particular, warps, which have a velocity signature similar to radial oscillations, remain a competitive model even where there is no visible evidence for warping. Nevertheless, given the theoretical prediction of radial oscillations in the embedding potential, we propose that current tilted-rings models for warped spirals are incomplete; adding to the fits a single free parameter per ring—the lowest-order (symmetric) radial velocity—would be a valuable improvement.

CHAPTER 1

INTRODUCTION

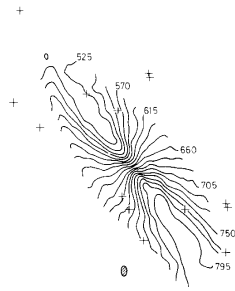
The image of spiral galaxies as flat, differentially rotating objects composed of matter moving on circular orbits has long been known to be oversimplified. While the visible portion of many spirals does conform reasonably well to this picture, virtually every disk galaxy ever observed extends far beyond what is observed optically. This extended component, largely composed of neutral hydrogen, is seen in the 21cm radio band and in most cases does not show the same kinematic behavior as the inner, visible part of the galaxy; that is, the outer regions of the galaxy tend to move somewhat differently from the inner regions, albeit usually with a smooth transition between the two—and usually in such a manner that a third component, a massive but invisible (dark) halo, is inferred. In many cases the HI component clearly does not even lie in the same plane as the visible component: the galaxy is warped.

Most spiral galaxies do not display a morphological warp, however. What they do tend to show is a systematic distortion in their velocity maps. Kinematic (Doppler) data are typically represented in contour form, and in the idealized case of planar circular orbits the plots possess a fourfold symmetry. But real galaxies are never ideal; their maps superimpose features due to underlying spiral structure, interactions with neighboring galaxies, and interactions with the surrounding dark halo. And since morphological warps unquestionably exist in *some* galaxies, it has become customary in the past two decades to try to interpret *any* symmetric distortion in terms of a warp.

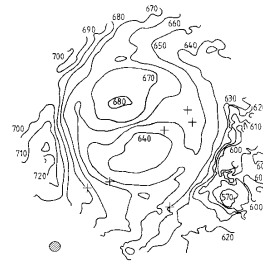
If the shape of the embedding gravitational potential is static, then warps are indeed the only plausible explanation of these symmetric distortions that are seen in so many velocity maps. But recent numerical experiments—fully self-consistent, long-duration, dynamical simulations of halo-like spheroidal systems—

Figure 1: **Velocity Maps for the Six Galaxies.** (a) NGC 3198. (b) NGC 628. (c) NGC 6503. (d) NGC 2403. (e) NGC 7331. (f) NGC 2903. Beam sizes are indicated by the shaded ovals. North is up; east is to the left. (NGC 628 is from Kamphuis and Briggs 1992; the others are from Begeman 1987.)

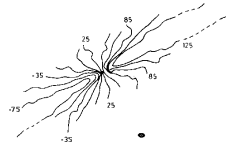
(a)



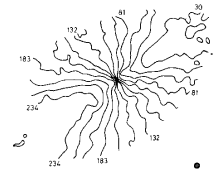
(b)



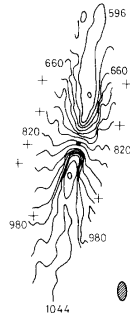
(c)



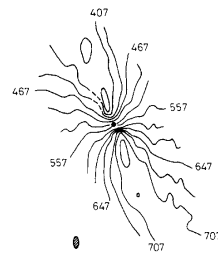
(d)



(e)



(f)



imply that the potential need not be static. On the contrary, it is quite possibly subject to normal modes and may therefore oscillate or “ring.” Such normal-mode oscillations in the galaxy’s background potential would tend to drag along the embedded disk, too, adding a radial component to its normally circular velocities. This suggests an alternative explanation for some of the kinematic distortions that are usually explained in terms of warps.

In this paper we look at half a dozen galaxies previously analyzed in terms of the warp model. Five of the galaxies were originally observed by Begeman and published in his thesis (1987, hereafter simply ‘Begeman’); the chapter on NGC 3198 was subsequently republished (Begeman 1989). The remaining galaxy, NGC 628, was observed by Kamphuis and Briggs (1992, hereafter ‘Kamphuis and Briggs’ or ‘KB’). Velocity maps for the six are shown in Figure 1. None of the galaxies shows evidence of morphological warping in the HI (although NGC 7331 does show an optical warp); we therefore ask whether there is observational evidence for radial oscillations, and if so, whether the magnitude of the oscillations is consistent with theoretical models. We also consider whether the data might provide any hints as to the modal structure of such oscillations. Note that the term “radial velocities” will be used throughout this paper to refer to those velocities associated with radial oscillations of a galaxy—that is, radial with an origin at the center of the galaxy under consideration. It does *not* refer to the line-of-sight, Earth-centered velocities sometimes also referred to as “radial.” Similarly, “radial fits” will be used informally to refer to models that include radial motions.

CHAPTER 2

THEORY

The motivation for pursuing this line of research is largely due to the numerical experiments of Miller and Smith (1994). In N-body calculations of 400,000 particles representing an isolated, stable, spherical galaxy with various but uniformly “quiet” initial conditions, long-term radial oscillations of reasonably large amplitude are seen. Miller and Smith argue that the oscillations represent normal-mode excitations of a stable galaxy.

Since these numerical galaxies are reasonable models of dark halos as well,¹ there is a strong possibility that many or most halos oscillate radially. And since flat rotation curves for spiral galaxies strongly imply a dark halo component at least 5 to 10 times as massive as the visible component, the halo dominates the gravitational potential in which the galaxy sits. Therefore a radially oscillating halo adds a radial component to the usual circular rotation of a disk galaxy.

That a radially oscillating, differentially rotating planar disk could produce the same sort of twisted velocity map as a warped disk was recognized as long ago as the late 1960’s by Shostak (1993), who tried first to explain peculiarities in observed maps by radial motions. At that time disk galaxies were thought to be stand-alone systems in the sense that the visible component was solely responsible for the gravitational potential, and since Lynden-Bell (1967) showed that such a system could not support normal modes of radial oscillation, Shostak later dropped his radial-motions model in favor of the now-popular tilted-rings approach.

Indeed, there is ample direct evidence for the existence and commonness of true warps (e.g., Bosma 1991), while the observational evidence for radial velocities

¹Their isolation is a notable exception to “reasonable”; but if anything, interactions between neighboring galaxy-halo pairs should excite oscillations.

consists largely of local or small-scale motions (e.g., Rubin et al. 1975a; Rubin et al. 1975b and 1977; etc.) and cases where a gaseous inflow makes sense (such as accretion onto a dense object in galactic nuclei). We are not aware of any high-resolution, minor-axis observations of highly inclined, non-morphologically warped disk galaxies; such studies would be the most obvious way to detect radial motions directly.

On the other hand, what Binney (1990) calls “the old warp puzzle” is still a potential problem. In a nutshell, the classical warp problem involves the observation that a simple warp (such as the so-called integral-sign warp) in a non-spherical potential should wind up rather quickly due to the effects of differential precession at various radii. But if this were the case, we should not see so many of the simple warps that we *do* see, both directly and indirectly. Sparke and Casertano (1988) have argued that a disk with a sharp enough edge in an oblate potential is subject to one or more discrete bending modes. Their analysis makes a number of large assumptions, however:

- The warp is one-dimensional in the sense that it has a constant line of nodes. Briggs (1990) has found that warped spirals tend to have a straight line of nodes (LON) only within the Holmberg radius (approximately); beyond that point—where the warp usually begins—the LON traces out a leading spiral. (He has also found that one can always choose an equatorial plane such that the line of nodes consists of two more-or-less straight segments, with the break occurring near R_{Holmberg} .) Christodoulou et al. (1993) looked at a sample of 15 galaxies and also found that the line of nodes is usually twisted.
- The galactic disk is a truncated exponential, tapering smoothly to zero surface density over a narrow region. This is not necessarily a poor assumption, but to our knowledge no spiral galaxy has ever been observed all the way to its edge; in every case, at the limits of detection the galaxy is still going strong (radially, that is). The Sparke-Casertano analysis finds that extending the

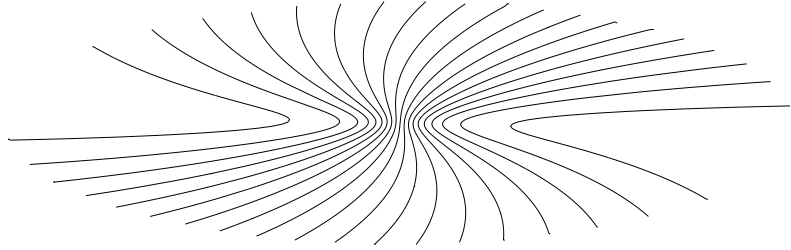
disk too far merges the discrete tilt mode into the continuum of warp modes. There is also the question of flaring, which is observed in the outer parts of some galaxies' HI envelopes (e.g., M31, discussed in Brinks and Burton 1984).

- The galactic halo is axially symmetric. It is not yet clear whether triaxiality would introduce an instability into Sparke and Casertano's analysis, but the possibility exists. In any case, as Binney (1992) points out, we don't particularly care if warps are not normal modes; it is sufficient that they be reasonably long-lived. The matter of a hypothetical instability then becomes a question of whether the actual deviation from axisymmetry is large enough to affect the warp on observable timescales. If the timescale of the instability were greater than a Hubble time, clearly the question would be moot.
- The halo is static (i.e., not dynamically self-consistent—a point that Sparke and Casertano themselves made). As Binney (1990 and 1992) notes, the central part of the halo will be coupled to the disk more closely than to the outer halo and must therefore be treated as a dynamical subsystem. And, of course, the whole point of Miller and Smith's (1994) paper is that a spheroidal system is dynamically very active.
- The effect of gas dynamics is ignored. In reality dissipation can be a large effect; consider the settling disk models of Steiman-Cameron and Durisen (1988 and 1990), as apparently directly observed in NGC 3718. Binney (1992) also notes that cosmic infall is expected to include some gas that will contribute to the transfer of angular momentum and that is likely to interact with gas at typical warp radii. Modelling gas dynamics in a gravitational field is both difficult and computationally expensive; nevertheless, it seems likely that gaseous effects play an important role in warp dynamics.

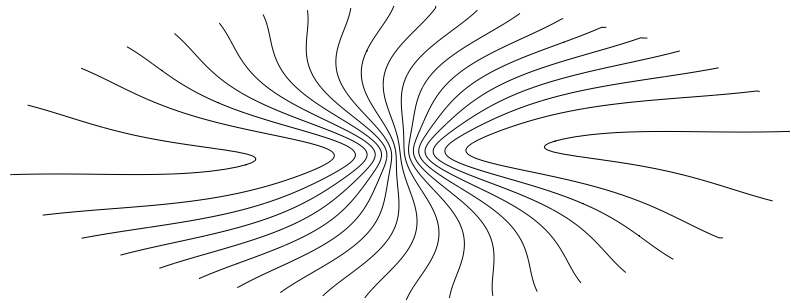
None of these points *necessarily* voids Sparke and Casertano's analysis, but taken collectively they imply that the question of warps' longevity is not yet entirely closed.

Figure 2: **Faked Velocity Maps.** As described in the text: (a) Planar model oscillating in the fundamental radial mode. (b) Planar model oscillating in a spherically symmetric radial mode with one node. (c) Warped model resulting from a tilted-rings fit to the velocity map in (b). The ‘squiggles’ at the ends of some of the contours in (c) are due to imperfect interpolation of the velocity field between the outermost rings.

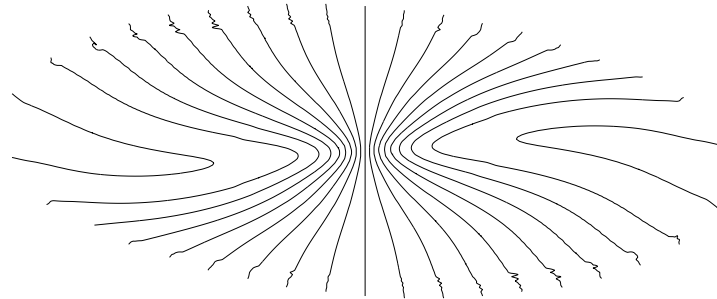
(a)



(b)



(c)



In addition, the possibility of large-scale radial oscillations is new enough that some of the lack of evidence may simply be due to the fact that no one has yet made a concerted effort to look for such things. The unfortunate truth is that they're hard to detect; the signatures are usually ambiguous and easily mistaken for other effects—including warps. Nevertheless, assuming for now the existence of a fundamental radial mode (a “breathing mode” in which the entire galaxy expands or contracts homologously, and the mode with the greatest amplitude and energy in the Miller-Smith experiments), what sort of velocities would be expected in a typical disk galaxy, and what do the corresponding velocity maps look like? In fact the magnitudes are quite interesting. For a disk galaxy of comparable size to our own, embedded in a spherical, dark halo of five to ten times the mass of the visible galaxy, typical velocities at the edge of the optical disk are 10 to 20 km/s, with a periodicity on the order of 3×10^8 yr. This being an homologous mode, the velocities increase linearly with radius and may therefore exceed 50 km/s toward the edge of the detectable neutral-hydrogen disk; but the maximum displacement at any radius is on the order of 5%.

Figure 2a shows the velocity map corresponding to a faked galaxy subject to this breathing mode. The circular (azimuthal) velocity approaches an asymptote of 150 km/s as R gets large, and the radial velocity grows linearly to 40 km/s at the outer edge. Qualitatively the map bears a strong resemblance to what one would expect from a warp.

Miller and Smith also detected a strong, spherically symmetric mode with a single radial node. This “second radial mode” had a period between one third and half of that of the fundamental mode and an amplitude comparable to it or even slightly larger. The second radial mode is particularly intriguing for the current study because of the velocity maps it produces. Figure 2b shows such a velocity map—generated from a completely flat model oscillating in a single-node radial mode. Figure 2c shows a velocity map generated from a standard tilted-rings model. The two are strikingly similar. They are clearly not mathematically degenerate, but

in practical cases—with superimposed spiral-arm “noise” and typical observational resolution—they very nearly are.

CHAPTER 3

PROCEDURE

The analysis described here is unusual in that it begins with a published velocity map rather than the raw channel-map data usually associated with HI (radio) observations. There were three reasons for this. In the first place it avoids the necessity of detailed knowledge of the observational equipment and of the data analysis required to clean the data of systematic effects; that is left to the expert who took the data. Second, it provides immediate access to data that otherwise might be difficult or impossible to acquire. Third, it was initially thought that the procedure would be fast enough to allow the analysis of perhaps a couple dozen galaxies, in turn allowing some results of a statistical nature. In fact, this last benefit was never realized; with software improvements it might be, but currently the tools are somewhat crude and labor-intensive.

Nevertheless, the procedure is workable and produces good results. It starts with a high-resolution scan of a velocity map. The scanned image is converted from bitmap format into lists of data points lying on each isovelocity contour (see Appendix A for details). Once the velocity data have been converted to this format and cleaned of tracing artifacts, they are fed into a fitting routine.

Like tilted-rings fitting programs, the radial-oscillations version models the galaxy as a set of concentric rings with both global and local (per-ring) parameters to be fitted; the programs differ in their choices of which parameters are allowed to vary. Both fit the systemic (or recessional) velocity of the galaxy and the position of its center as global values, and they fit the rotation velocity of each ring individually. But where tilted-rings programs also fit the inclination and position angle¹ of each

¹Begeman's fits, KB's and ours all use the inclination of the ring relative to the observer's line

	Tilted Rings	Radial Flows	
		$m = 0$	$m = 2$
Global	systemic velocity v_{sys} center (x_0, y_0)	systemic velocity v_{sys} center (x_0, y_0) inclination i position angle ϕ	
Local (per ring)	rotation velocity v_c inclination i position angle ϕ	rotation velocity v_c radial velocity $v_r^{(0)}$	rotation velocity v_c $m = 0$ radial velocity $v_r^{(0)}$ $m = 2$ radial velocity $v_r^{(2)}$ $m = 2$ phase φ_0

Table 1: **Comparison of Fitting Parameters for the Three Models.**

ring individually, the radial-motions fits make these global. In their stead the zeroth-order radial velocity of each ring is varied (two-parameter fit; the circular velocity is the other parameter). Optionally the second-order radial velocity and corresponding phase—that is, the term corresponding to the $l = 0, m = 2$ spherical harmonic—of each ring may also be allowed to vary (four-parameter fit). The $l = 0, m = 1$ mode corresponds to translation of the ring (“sloshing”) and is disallowed. The second-order circular velocity, analogous to the second-order radial velocity, is likewise disallowed since the rings would have to be ellipses to accommodate such flows. Table 1 summarizes the parameters in each fit.

As an aside, it is worth pointing out here that, although we refer to “two-parameter,” “three-parameter” and “four-parameter” fits throughout this paper, these refer to the number of parameters *per ring*. The tilted-rings fit, for example, has three free parameters for each ring, but its total number of free parameters is $3N + 3$, where N is the number of rings. The “two-parameter” radial fit, on the other hand, has a total of $2N + 5$ free parameters ($N - 2$ fewer than tilted rings).

of sight and the position angle of the receding half of the major axis on the sky (measured counter-clockwise from the north), but one could equally well use parameters relative to the remote galaxy instead (for example, inclination relative to some fiducial “galactic plane” and the longitude of ascending node).

The equation for the tilted-rings model is

$$v_{\text{obs}}(\vec{\mathbf{r}}) = v_{\text{sys}} - v_c \sin i \cos \varphi(\vec{\mathbf{r}}), \quad (3.1)$$

while that for the radial-motions model is

$$v_{\text{obs}}(\vec{\mathbf{r}}) = v_{\text{sys}} - \sin i \left[v_c \cos \varphi(\vec{\mathbf{r}}) + \left(v_{\text{r}}^{(0)} + v_{\text{r}}^{(2)} \cos(2\varphi(\vec{\mathbf{r}}) + \varphi_0) \right) \sin \varphi(\vec{\mathbf{r}}) \right]. \quad (3.2)$$

In these equations $\vec{\mathbf{r}}$ represents the position on the sky of a given point, $v_{\text{obs}}(\vec{\mathbf{r}})$ is the observed (line-of-sight) velocity at that point, and $\varphi(\vec{\mathbf{r}})$ is the azimuthal angle in the plane of the galaxy between the observed point and the fiducial line defined by the position angle (along the receding half of the major axis). The remaining variables are either the global or per-ring fitted parameters: v_{sys} is the systemic velocity of the galaxy, v_c is the circular velocity, $v_{\text{r}}^{(0)}$ and $v_{\text{r}}^{(2)}$ are the zeroth-order and second-order radial velocities, i is the inclination, and φ_0 is the phase corresponding to the second-order radial velocity.

The azimuthal angle φ is defined by the equations

$$\cos \varphi(\vec{\mathbf{r}}) = \frac{(x - x_0) \sin \phi - (y - y_0) \cos \phi}{R(\vec{\mathbf{r}})} \quad (3.3)$$

$$\sin \varphi(\vec{\mathbf{r}}) = \frac{(x - x_0) \cos \phi + (y - y_0) \sin \phi}{R(\vec{\mathbf{r}}) \cos i}, \quad (3.4)$$

in which the sky coordinates $(x, y) \equiv \vec{\mathbf{r}}$ appear explicitly. (x_0, y_0) is the position of the center of the galaxy, and ϕ is the position angle. $R(\vec{\mathbf{r}})$ is the radius in the plane of the galaxy, given by

$$\begin{aligned} R &= |\sin \phi| \sqrt{c_{xx}x^2 + c_{xy}xy + c_{yy}y^2 + c_x x + c_y y + c_0} & (3.5) \\ c_{xx} &= 1 + \cot^2 \phi \sec^2 i \\ c_{xy} &= 2 \cot \phi (\sec^2 i - 1) \\ c_{yy} &= \cot^2 \phi + \sec^2 i \end{aligned}$$

$$\begin{aligned}
c_x &= -2c_{xx}x_0 - c_{xy}y_0 \\
c_y &= -2c_{yy}y_0 - c_{xy}x_0 \\
c_0 &= c_{xx}x_0^2 + c_{xy}x_0y_0 + c_{yy}y_0^2.
\end{aligned}$$

The requirement to fit both local and global parameters means that the fitting program is doubly iterative: it is not sufficient merely to converge to a best fit for each ring, followed by a best fit for the global parameters; since the individual ring fits *depend* on the global parameters, they must be redone whenever the global parameters change significantly. In turn, the globals depend on the individual ring parameters, so they too must be refit. This “superiteration” of individual rings plus globals fits, each of which is itself an iterative process, is continued until overall convergence is achieved. At the lowest levels of iteration the nonlinear least-squares method of Levenberg and Marquardt, as implemented by Press et al. (1992), was used.

We also found it necessary to write a tilted-rings fitting program in addition to the main radial-oscillations program described above. There were two principal reasons for this: to allow for a more direct comparison of tilted-rings and radial fits, and to provide an additional check and error estimate on the overall method of fitting to a published velocity map. For example, the literature includes residuals maps for only four of the galaxies, and an overall root-mean-square (RMS) residual—a crude but useful “one-number” metric for goodness-of-fit—was provided for none of them.

CHAPTER 4

RESULTS

4.1 Faked Galaxies

As a direct test of the level of degeneracy between the velocity maps of warped galaxies and radially oscillating ones, and as a way to verify that our fitting routines were functioning correctly, a pair of radial-motions models was created and fed back into both routines. The first faked galaxy was subject to the fundamental breathing mode; it was given a circular velocity of 150 km/s, and its zeroth-order radial velocity grew linearly from zero at the center to 40 km/s at its outer edge. The corresponding velocity map is shown in Figure 2a and not only shows the classic twist in contours along the major axis but also a distinctive S-shape in the minor-axis contours. The PostScript form of this map was used as input to the fitting routines, simulating the scan-based approach used for the real galaxies. Figures 3a and 3b show the results of the radial-motions fit; clearly the model parameters have been recovered to near perfection, as confirmed by the overall RMS residual of 0.02 km/s. (The residual would have been even lower had the fit not been cut short for lack of interest.) The residuals map consists of a few specks and is not shown here due to poor photo-reproducibility.

The tilted-rings fit, on the other hand, was quite poor. Figures 3c–3f show the results. With the exception of the four outermost rings, the circular velocity (Figure 3c) is recovered nicely, and the inclinations and position angles (Figures 3d and 3e) both undergo a fairly dramatic change over the range of fitted radii but still an entirely reasonable one. The residuals map in Figure 3f, however, tells a different story. The four outermost rings apparently “fell off” the outer edge of the contours early in the fitting procedure and then proceeded to rotate to some

improbable orientation. (Note that this is due to a limitation in our tilted-rings fitting program and did not occur for any of the other galaxies.) Even ignoring the outer four rings, the inner residuals are almost uniformly large, with an RMS value of more than 8 km/s.

The second faked galaxy was loosely based on results from radial fits of the actual galaxies discussed below. Instead of the linear radial mode used in the first example, a one-node sinusoidal “mode” with an amplitude of 15 km/s was chosen. The node was placed at approximately 75% of the maximum radius, and the resulting velocity field is shown in Figure 2b. It is interesting to note that the bends in the contours are somewhat suggestive of a two-armed spiral. As in the previous case the PostScript data were fed to the radial-motions fitting program, with similarly excellent results (Figures 4a and 4b). Unlike the previous test, however, the tilted-rings fit was also quite good (Figures 4c–4f). Virtually the same rotation curve is recovered as in the radial fit; and while the inclinations show a mild variation as a function of radius (Figure 4d), the position angles plunge rather more dramatically. The real beauty lies in the residuals map, however (Figure 4f). At all points but the outermost edge the residual is under 10 km/s, and the overall RMS residual is only 4.1 km/s—a very good result. This latter point is worth emphasizing: in a galaxy with no warp at all, the tilted-rings model produces what would normally be considered an excellent fit.

In order to “close the circle,” a velocity map corresponding to the final tilted-rings model was created; this is what is shown in Figure 2c. It is apparent that, although the two maps match fairly well along the major axis, along the minor axis they are quite distinct: the central contour in the tilted-rings case is completely straight, while that in the original radial-oscillations map (Figure 2b) is integral-shaped. On the other hand, distortions from spiral structure could conceivably reproduce much of the waviness in the original map.

Figure 3: **Faked Planar Galaxy Oscillating in the Fundamental Radial Mode.** (a) Two-parameter radial fit, circular velocity. (b) Two-parameter radial fit, zeroth-order radial velocity. (c) Tilted-rings fit, circular velocity. (d) Tilted-rings fit, inclinations. (e) Tilted-rings fit, position angles. (f) Tilted-rings fit, residuals map; RMS residual is 8.4 km/s. Note that the four outermost rings in the twisted-rings fit have ‘fallen off’ the contours and twisted around unrealistically. Dotted horizontal lines in (a)-(c) are for reference only.

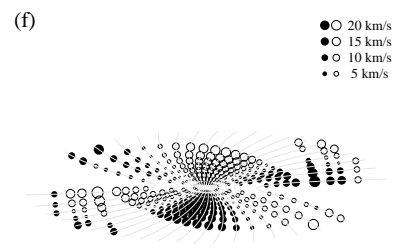
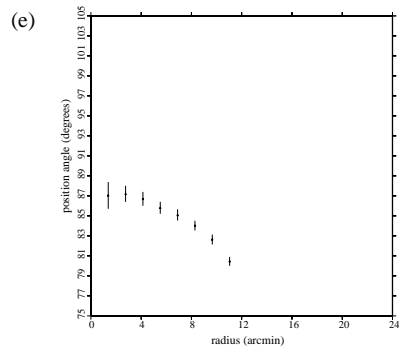
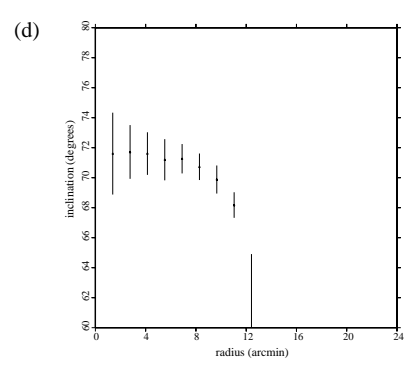
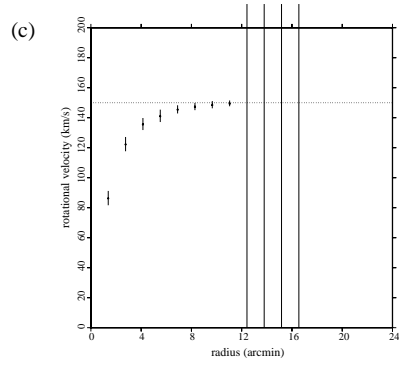
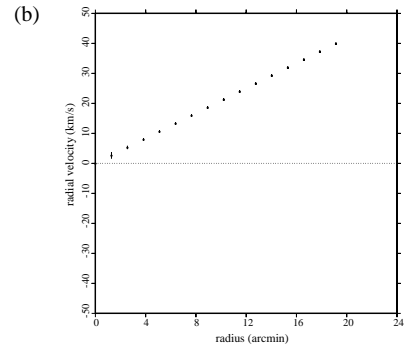
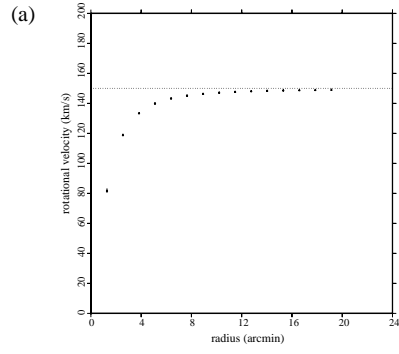
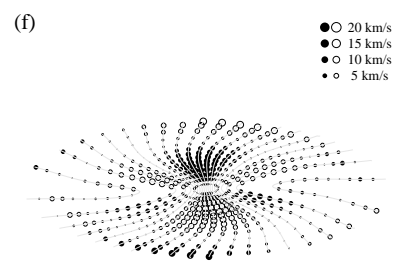
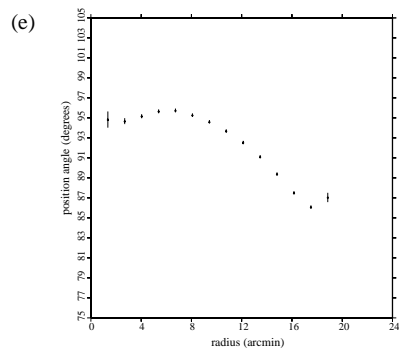
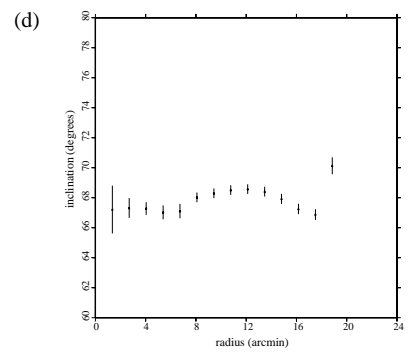
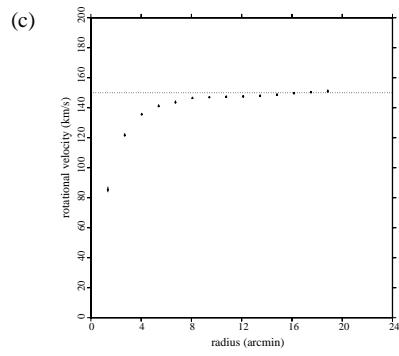
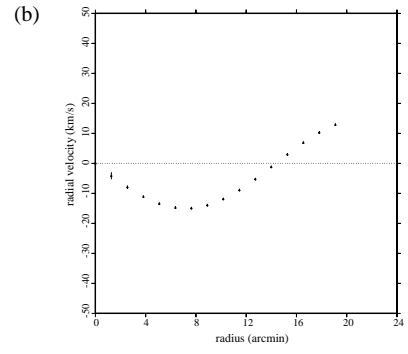
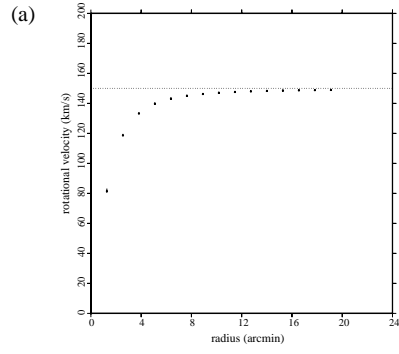


Figure 4: **Faked Planar Galaxy Oscillating in a Single-Node Radial Mode.** (a) Two-parameter radial fit, circular velocity. (b) Two-parameter radial fit, zeroth-order radial velocity. (c) Tilted-rings fit, circular velocity. (d) Tilted-rings fit, inclinations. (e) Tilted-rings fit, position angles. (f) Tilted-rings fit, residuals map; RMS residual is 4.1 km/s. Note the threefold azimuthal symmetry in the residuals map. The horizontal lines in (a)-(c) are only for visual reference.



4.2 NGC 3198

NGC 3198 is classified a type Sc(rs)I-II (Sandage and Tammann 1981) and has very clean, symmetric contours (Figure 1a). It is also remarkable for its rotation curve that extends to 11.4 exponential scale lengths, one of the farthest of any galaxy observed to date (van Albada et al. 1985). (The scale length is defined in terms of the optical disk.) Aside from the obvious twist in the contours—extending from the central region all the way to either end of the major axis—the only other features of note are a set of coherent ripples strongly correlated with the spiral structure. This being the case, one would expect any reasonable model to do fairly well, possibly excepting the regions where the spiral structure is most obvious.

The radial-velocity fits are in fact quite good. The rotation curves for both two-parameter and four-parameter fits are very similar to the one Begeman derived in his tilted-rings fit (Figures 5a and 5c, respectively; the solid rotation curve is Begeman’s). This is not surprising given the source of the data used in the present analysis. More interesting are the radial-velocity curves, shown in Figures 5b and 5d–5f. Not only are the velocity magnitudes very reasonable for this model, the correlation between rings of similar radii is very high—that is, the curves of radial velocity vs. radius are amazingly smooth.

On the other hand, the four-parameter fit shows a disturbing tendency to improve the fit results by balancing large velocities. That is to say, where the two-parameter fit performs quite well with radial velocities of absolute value less than 7 km/s, the four-parameter fit requires magnitudes of more than 10 km/s for both zeroth-order and second-order radial velocities. This is not necessarily a horrible thing, but it suggests that the improvements in the four-parameter fit are solely due to having two extra degrees of fitting freedom per ring, rather than reflecting anything about the underlying physics of the galaxy.

And the residuals are indeed excellent. The root-mean-square residual for the two-parameter model is 3.6 km/s; for the four-parameter fit it is 3.2 km/s. This

compares well with the RMS residual of 3.5 km/s from our own tilted-rings fit, which was intended to duplicate Begeman’s ROTCUR fit. Figure 6 shows the maps of the residuals for the three fits. Open circles indicate that the model velocities are greater than observed; filled circles indicate the reverse. The *area* of each circle is proportional to the magnitude of the difference at that point, so that if the residual at point A is twice as big as that at point B, the dot at point A will be twice as big—not four times as big, as would be the case if the *radii* were proportional to the velocity differences. Thus the actual results should closely approximate the overall visual/intuitive “feel” of the map.

Begeman’s published residuals are presented in such a way that they are difficult to compare with the map in Figure 6c, but the two appear to be consistent with each other. (We are, of course, well aware of Press et al.’s (1992) comments with respect to “chi by eye.”) More to the point, the tilted-rings circular velocity matches extremely well (Figure 7a). Surprisingly the plots of inclinations and position angles, while superficially similar, are not equally good matches. In particular, the inclinations differ qualitatively; ours drop from 72.5° to 70° at $1.5'$ and remain fairly constant out to $8'$, where Begeman’s rise steadily from 70° at $5'$ to 75° at $9'$. The position angles match better—both peaking at $2'$ and declining steadily by about 5° out to $8'$ —but the comparison is impeded by the fact that our fit of NGC 3198 is not corrected for the possible rotation of the original figure when it was scanned (which would result in a shift of the position angles by a constant). Both comparisons are also muddled by the fact that Begeman fit the northern and southern halves of the galaxy separately, and, while the agreement between the halves is reasonable, it is by no means perfect. His adopted curves, on the other hand, are artificially smooth.

In short, NGC 3198 does not provide a good test of the scan-based tilted-rings fitting method; some of the results match well but the others poorly, leaving the overall comparison somewhat ambiguous. Fortunately the other galaxies provide a cleaner check on the method.

Figure 5: **NGC 3198 Radial Fits.** (a) Two-parameter fit, circular velocity. (b) Two-parameter fit, zeroth-order radial velocity. (c) Four-parameter fit, circular velocity. (d) Four-parameter fit, zeroth-order radial velocity. (e) Four-parameter fit, second-order radial velocity. (f) Four-parameter fit, phase of second-order radial velocity. The solid curve in (a) and (c) is Begeman's, and the horizontal lines are for reference only.

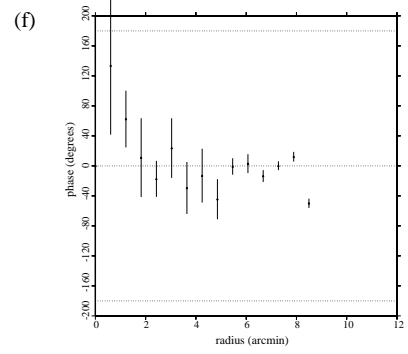
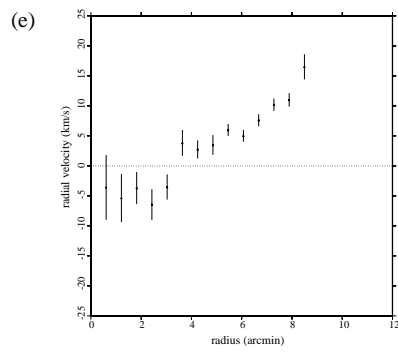
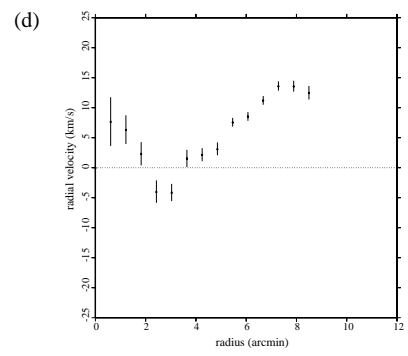
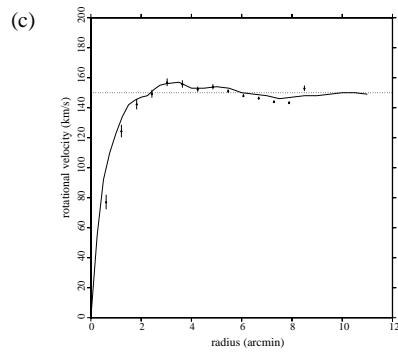
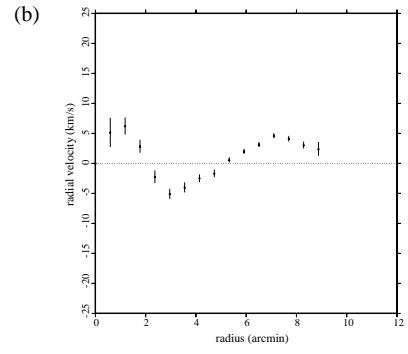
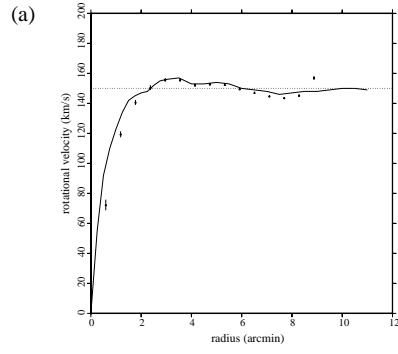


Figure 6: **NGC 3198 Residuals.** (a) Tilted-rings fit; RMS residual is 3.5 km/s. (b) Two-parameter radial fit; RMS residual is 3.6 km/s. (c) Four-parameter radial fit; RMS residual is 3.2 km/s.

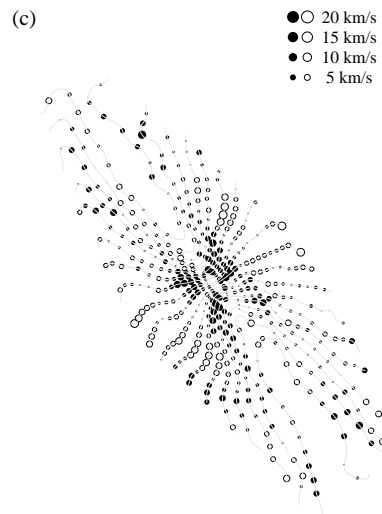
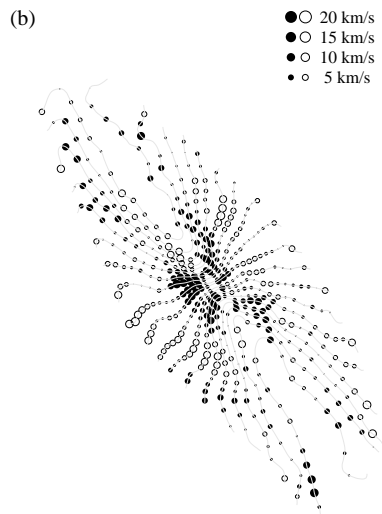
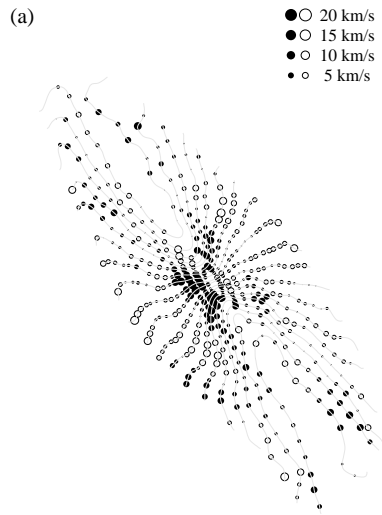
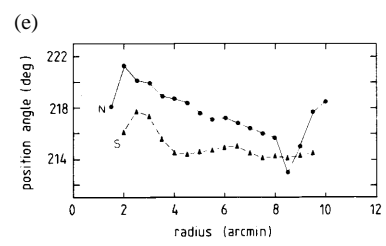
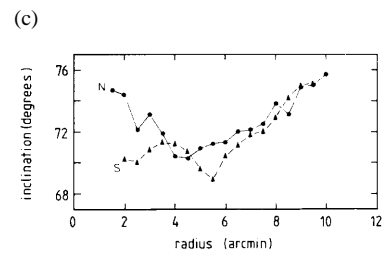
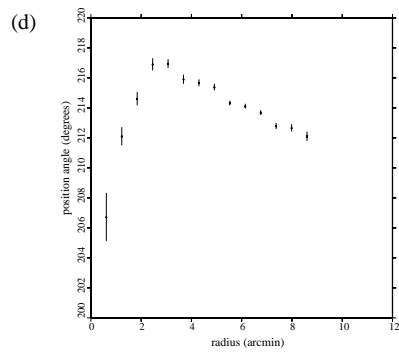
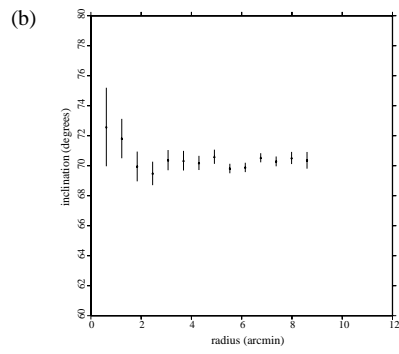
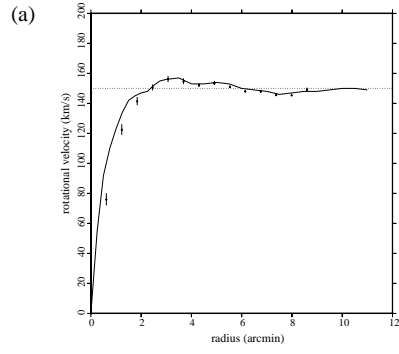


Figure 7: **NGC 3198 Tilted-Rings Fits.** Our fits are on the left; Begeman's are on the right, except as noted. (a) Circular velocities; the solid rotation curve is Begeman's fit, and the horizontal line is for reference only. (b), (c) Inclinations. (d), (e) Position angles.



4.3 NGC 6503

NGC 6503 is a type Sc(s)II.8 spiral (Sandage and Tammann 1981). Its velocity map is almost perfectly symmetric and shows no visible indication of a warp or radial motions. The galaxy is particularly notable for its rotation curve, which Begeman derives to a distance of 12.9 scale lengths—even farther than NGC 3198—and which is completely flat for the entire distance.

Our tilted-rings fit reproduces Begeman’s rotation curve quite closely over the tested range of radii (Figure 8a). Unfortunately, said range is only about two-thirds of the range of the original data. This is a drawback of the scan-based data acquisition method: a minimum number of contours must be present at each radius. In the case of NGC 6503, large-radius data are only available along the major axis. With original data this is a near-ideal situation, at least for determining the rotation curve; for a velocity-map-based analysis, it works less well. The reason for this is that the major axis is where the best original data are taken, so the fits can still be quite good; but in the second-hand velocity-map analysis, where only the contours are available, typically only two to four data points are available for fitting. A fit can still be done with a minimum of four points, but the fitting errors are large. Fewer than four points is hopeless.

Nevertheless, as noted, our circular-velocity fit over the available range is a nearly perfect match to Begeman’s curve. The inclinations (Figures 8b and 8c) are also quite good, with virtually every feature reproduced accurately. Note that Begeman’s angular fits extend only from $2'$ to $10'$, while ours extend to $9'$; the ranges are much closer than for the circular-velocity fits. For the position angles (Figures 8d and 8e) the agreement is again very good, although the final “step” between $9'$ and $10'$ in Begeman’s fits (at -61°) is not present in our fit due to the limited radial range. Overall, however, the match between the fits is excellent support for the validity of the scan-based analysis method, particularly given the very high inclination of the galaxy.

As an aside, note that Begeman claimed on the basis of his fit that there is no evidence of a warp; we disagree. The position angle is measured on the sky, as a projected angle, not in the galaxy's frame of reference. For a highly inclined galaxy like NGC 6503, a small change in position angle translates into a large change in ring orientation in the galaxy's frame. Since the position-angles curve in both Begeman's fit and ours is smooth and shows a distinct downward trend, we claim that, if the tilted-rings model is to be believed, it is strongly suggestive of a moderate warp.

Not surprisingly, the radial-velocity model also reproduces Begeman's circular velocities quite closely over the tested range of radii (Figures 9a and 9c). The radial velocities are more interesting. Figure 9b shows the plot of angle-independent radial velocities. The data are beautifully self-consistent in the sense of having virtually no scatter at all, with the exception of the outermost ring. The plot is also interesting in that there is apparently no radial motion at all out to $R = 6'$. Beyond $6'$ the galaxy appears to have a small inward radial component of roughly 5 km/s.

The four-parameter radial fit produced a similar plot for the zeroth-order (angle-independent) radial velocity, which one would expect of a slightly more refined model. The second-order radial velocity curve, however, is not only of comparable or greater magnitude out to $8'$ or $9'$ but rises dramatically beyond that radius. It is apparently compensated by a drop in the circular velocity at the same point. As with NGC 3198, this behavior of balancing unexpectedly large velocities (or small ones, in the case of the rotation curve) suggests that the four-parameter fit is not telling us anything physical.

The residuals maps for NGC 6503 (Figure 10) do not differ strikingly from each other. This is another indication of the near degeneracy between tilted-rings and radial-velocities models, particularly for a galaxy with symmetric velocity contours. The overall residuals are quite small: 3.7 km/s for the tilted-rings fit, and 3.9 km/s and 3.2 km/s for the two radial fits.

Figure 8: **NGC 6503 Tilted-Rings Fits.** Our fits are on the left; Begeman's are on the right, except as noted. (a) Circular velocities; the solid rotation curve is Begeman's fit, and the horizontal line is for reference only. (b), (c) Inclinations. (d), (e) Position angles.

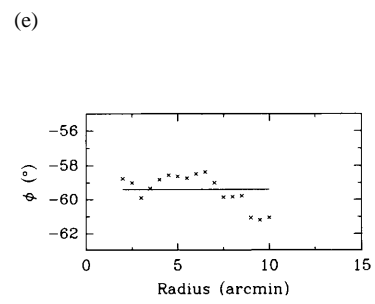
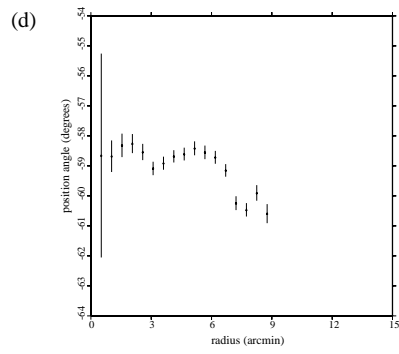
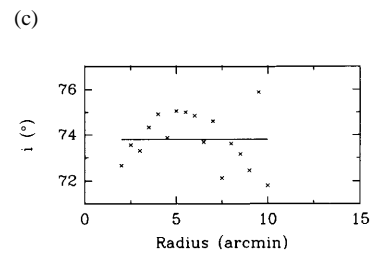
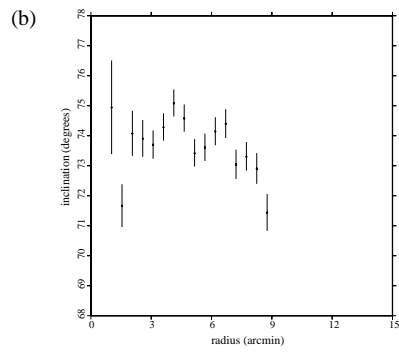
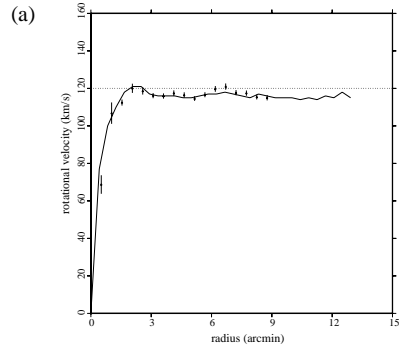


Figure 9: **NGC 6503 Radial Fits.** (a) Two-parameter fit, circular velocity. (b) Two-parameter fit, zeroth-order radial velocity. (c) Four-parameter fit, circular velocity. (d) Four-parameter fit, zeroth-order radial velocity. (e) Four-parameter fit, second-order radial velocity. (f) Four-parameter fit, phase of second-order radial velocity. The solid curve in (a) and (c) is Begeman's, and the horizontal lines are for reference only.

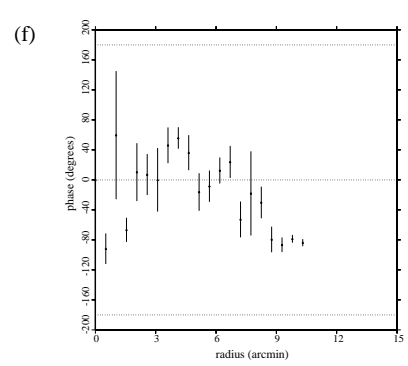
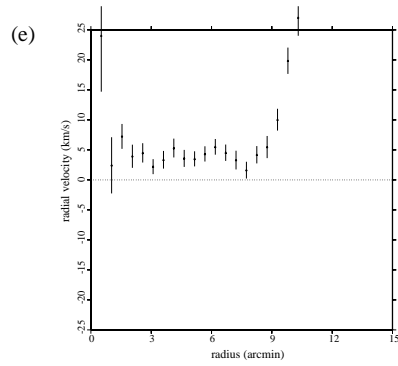
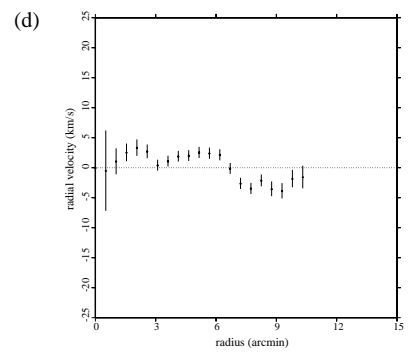
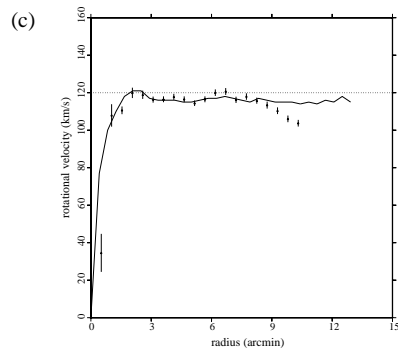
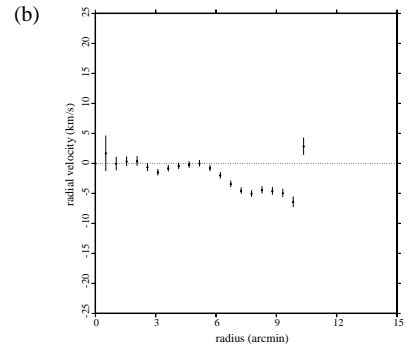
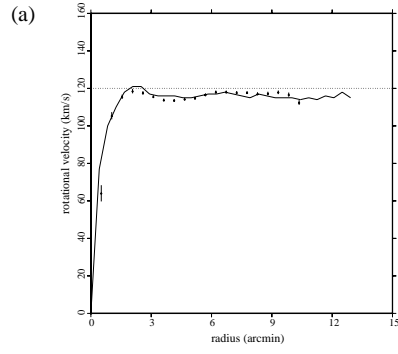
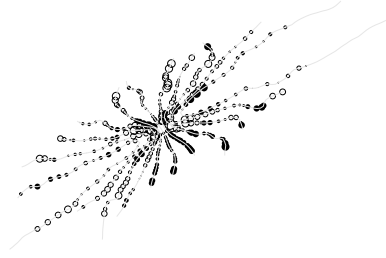


Figure 10: **NGC 6503 Residuals.** (a) Tilted-rings fit; RMS residual is 3.7 km/s. (b) Two-parameter radial fit; RMS residual is 3.9 km/s. (c) Four-parameter radial fit; RMS residual is 3.2 km/s.

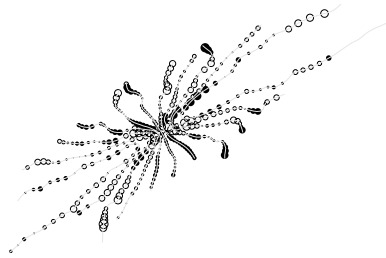
(a)

- 20 km/s
- 15 km/s
- 10 km/s
- 5 km/s



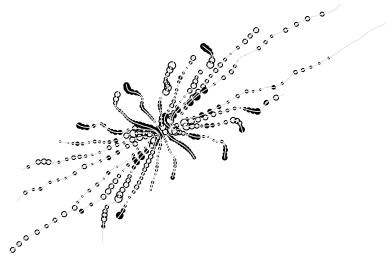
(b)

- 20 km/s
- 15 km/s
- 10 km/s
- 5 km/s



(c)

- 20 km/s
- 15 km/s
- 10 km/s
- 5 km/s



4.4 NGC 2403

NGC 2403 is a type Sc(s)III spiral (Sandage and Tammann 1981) at a lower inclination than 3198 and 6503 and with somewhat less clean contours. At least some of the ripples seem related to the spiral structure.

As with the previous two galaxies, the tilted-rings fit reproduces Begeman’s rotation curve very nicely (Figure 11a). The inclinations (Figures 11b and 11c) also match reasonably well, with most of the same peaks and valleys at the same radii, but Begeman’s fit shows more scatter and somewhat lower inclinations at large radii ($R > 12.5'$). To some extent the differences may be *due* to the scatter; it implies that the choice of ring radii may have a large influence on the fit results. That would not explain the 2° – 3° difference in the outer regions, however.

The fitted position angles (Figures 11d and 11e) also differ somewhat, both qualitatively and quantitatively. Not counting the inner $4'$ (omitted in Begeman’s plots), the average position angle is between 122° and 123° in the original fit and roughly 125° in the current one. Since the scan-based data for NGC 2403 (and, indeed, for all of the current sample except NGC 3198) were corrected for scan rotation, there is no obvious explanation for this offset. Our plot is also smoother between $4'$ and $12'$; again, no explanation presents itself.

Both radial-velocities fits reproduce Begeman’s rotation curve well (Figures 12a and 12c). The derived radial velocities themselves are much more interesting, particularly in the two-parameter case (Figure 12b). The correlation between adjacent rings is high—that is, the curve is smooth—and the velocities are completely reasonable for the model: consistently positive and under 10 km/s. For the four-parameter case the zeroth-order radial velocity curve (Figure 12d) is gratifyingly similar to the two-parameter case, although there is somewhat more scatter, and the second-order radial velocities are mostly of lesser magnitude except below $4'$. On the other hand, both the second-order velocities and the corresponding phases show a fair amount of scatter. It is hard to believe that they reflect a real behavior

in the galaxy dynamics.

The residuals for the NGC 2403 fits are a little larger than those for NGC 3198 and NGC 6503, but they are still good: 4.0 km/s for both the (three-parameter) tilted-rings and two-parameter radial fits, and 3.7 km/s for the four-parameter radial fit. Figure 13 shows the three maps. (Begeman's tilted-rings map shows the same features as ours.)

Figure 11: **NGC 2403 Tilted-Rings Fits.** Our fits are on the left; Begeman's are on the right, except as noted. (a) Circular velocities; the solid rotation curve is Begeman's fit, and the horizontal line is for reference only. (b), (c) Inclinations. (d), (e) Position angles.

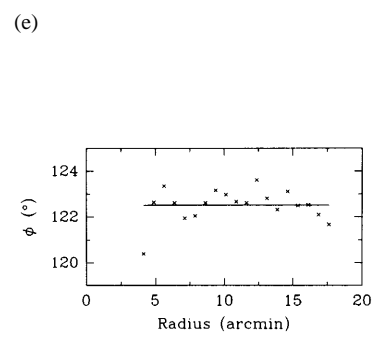
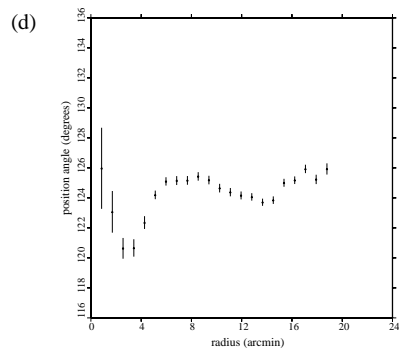
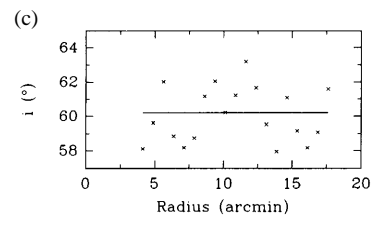
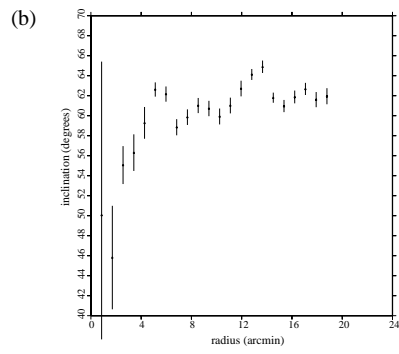
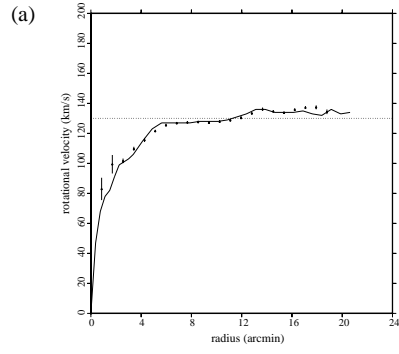


Figure 12: **NGC 2403 Radial Fits.** (a) Two-parameter fit, circular velocity. (b) Two-parameter fit, zeroth-order radial velocity. (c) Four-parameter fit, circular velocity. (d) Four-parameter fit, zeroth-order radial velocity. (e) Four-parameter fit, second-order radial velocity. (f) Four-parameter fit, phase of second-order radial velocity. The solid curve in (a) and (c) is Begeman's, and the horizontal lines are for reference only.

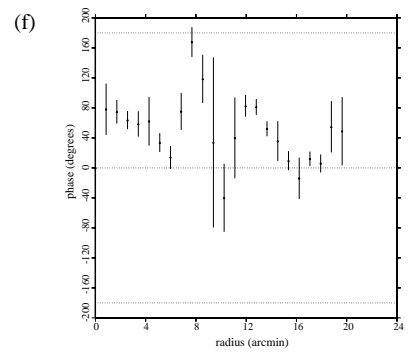
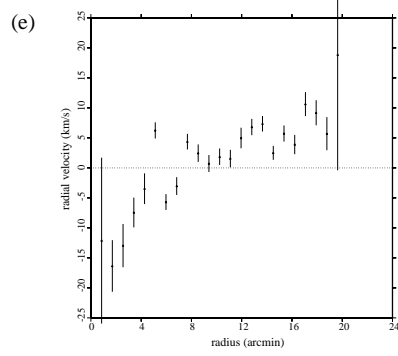
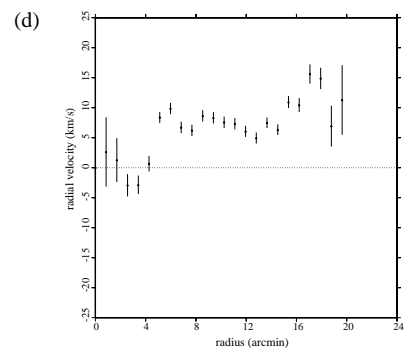
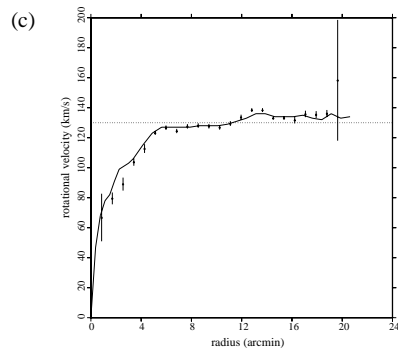
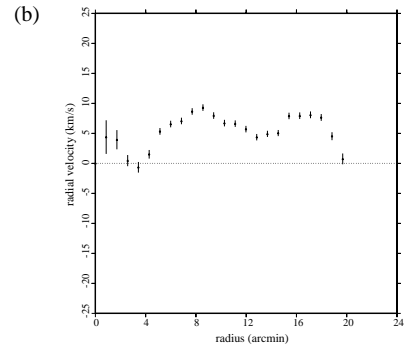
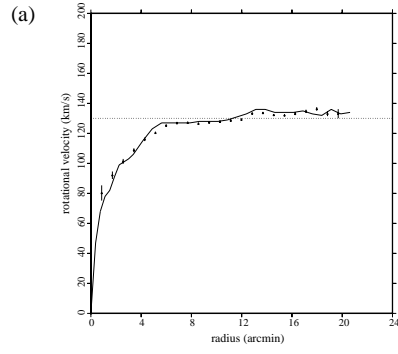
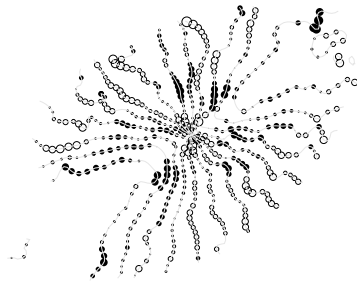
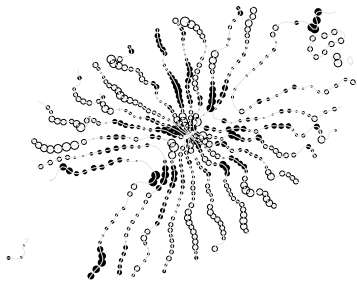
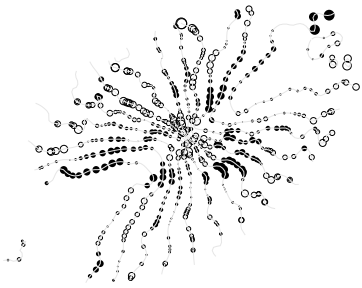


Figure 13: **NGC 2403 Residuals.** (a) Tilted-rings fit; RMS residual is 4.0 km/s. (b) Two-parameter radial fit; RMS residual is 4.0 km/s. (c) Four-parameter radial fit; RMS residual is 3.7 km/s.



4.5 NGC 7331

NGC 7331 is a type Sb(rs)I-II spiral (Sandage and Tammann 1981). Like NGC 3198 and NGC 6503, it is rather highly inclined. Unlike them, it has a luminous bulge component (Arp and Kormendy, 1972) and a much less symmetric velocity map. Most important, it has an outer dust lane that is clearly inclined relative to the inner region of the galaxy (as seen in the Hubble Atlas photograph). Thus one would not expect the radial-velocity model to fit the galaxy as well as the warp model.

Begeman’s separate fits of the approaching and receding halves of the galaxy found differences as large as 25 km/s, leading him to predict, “deviations from circular motion of at least 10 to 15 km/s may be present.” In the absence of the optical warp this might have sounded like an excellent lead-in for radial motions, but even in that case the near degeneracy of the two models would have come back to haunt the radial fit: it is as poor as the tilted-rings fit.

Figure 14 shows the residuals maps for the tilted-rings fits (including Begeman’s version) and both radial fits. All three are quite poor: the RMS residuals are 12.5 km/s, 13.5 km/s and 11.2 km/s for the tilted-rings, two-parameter radial and four-parameter radial fits, respectively. This is roughly three to four times as large as the residuals in the previous three galaxies. Moreover, individual differences exceed 20 km/s in some places.

The structure of the residuals is interesting, however; all three maps are clearly broken into roughly concentric zones of over- and underestimation. Begeman’s residuals map displays roughly the same structure, although it is more difficult to visualize given his choice of contour shading. This unique structure might imply a radially symmetric “hat-brim” warp mode oscillating along the axis, but it seems more likely that the bulge component is somehow responsible. Either way, it is clear that the radial-oscillations model does not provide an outstanding fit to the data.

Nevertheless, the fit results are worth looking at. The tilted-rings fit suf-

fers from a truncated range, somewhere between half and two-thirds of Begeman’s. Partly this is due to the galaxy’s very high inclination and the outer three rings’ “falling off” at the edge of the contours, but mostly it is due to the fact that the contours of the velocity map do not cover the full range of HI data. This is another limitation of the scan-based method. Even so, all three curves match Begeman’s extremely well over the available range: the circular velocities, not surprisingly (Figure 15a); the inclinations, starting at 75° and rising to 77° by $4'$ (Figures 15b and 15c); and the position angles, starting flat at 167° and then rising between $2'$ and $3'$ to a plateau at 172° (Figures 15d and 15e).

As with the other galaxies, the two-parameter radial results are fairly interesting, with the radial velocities lying on a near sinusoid with two radial nodes, one at $3'$ and the other at $5'$ (Figure 16b). The four-parameter fit echoes this shape but exaggerates it by more than a factor of two (Figure 16d), to be compensated by similarly large velocities in the second-order radial velocity curve (Figure 16e). As previously noted, this is not particularly believable, especially in light of the magnitude of the velocities (as high as 50 km/s) and the poor overall fit (11.2 km/s RMS residual). It is, however, interesting to note that the corresponding phases (Figure 16f) vary almost linearly from 0° to -180° as a function of radius; this, of course, is the definition of a spiral. Also note that the radial nodes appear to be in direct correspondence with the concentric zones mentioned above, an effect that is most noticeable along the eastern side of the galaxy in Figures 14b and 14c. Where the residuals are positive (i.e., model velocities are greater than observed: open circles), the zeroth-order radial velocities are negative; and vice versa where the residuals are negative (filled circles, positive radial velocities).

Figure 14: **NGC 7331 Residuals.** (a) Tilted-rings fit; RMS residual is 12.2 km/s. (b) Two-parameter radial fit; RMS residual is 13.5 km/s. (c) Four-parameter radial fit; RMS residual is 11.2 km/s. The outermost dots in (b) and (c) are at a radius of approximately $6'$.

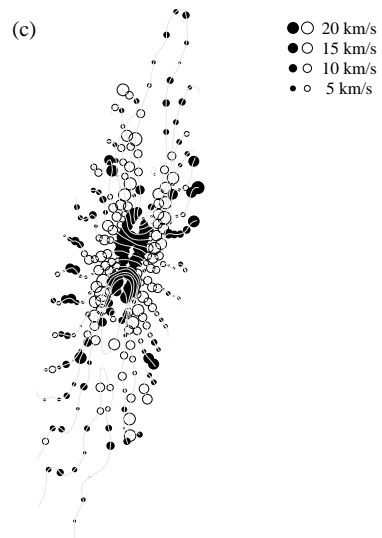
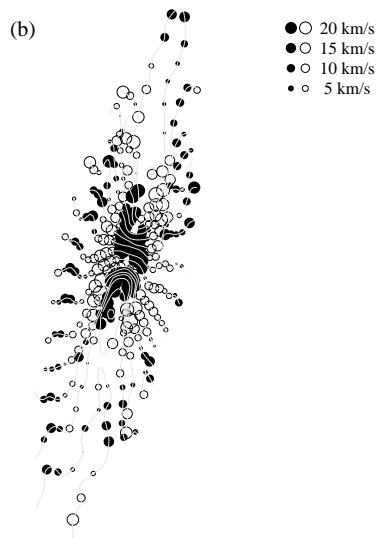
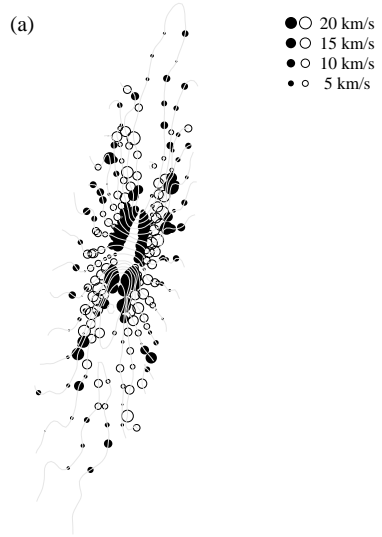


Figure 15: **NGC 7331 Tilted-Rings Fits.** Our fits are on the left; Begeman's are on the right, except as noted. (a) Circular velocities; the solid rotation curve is Begeman's fit, and the horizontal line is for reference only. (b), (c) Inclinations. (d), (e) Position angles.

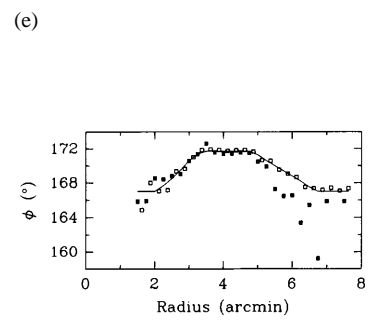
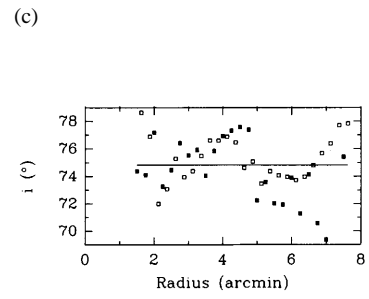
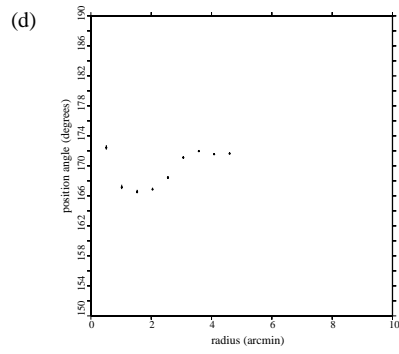
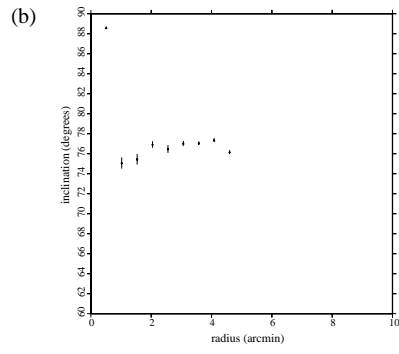
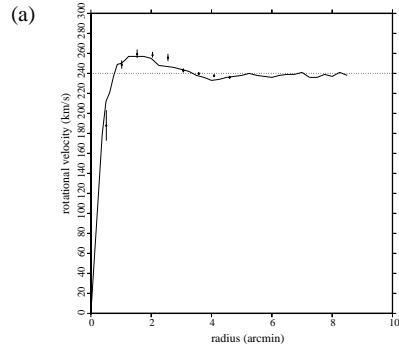
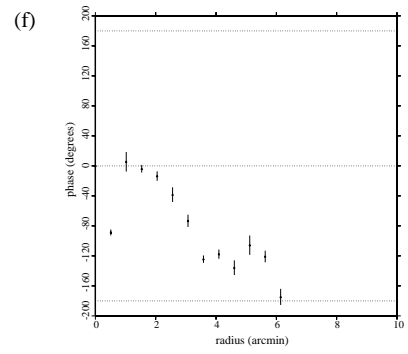
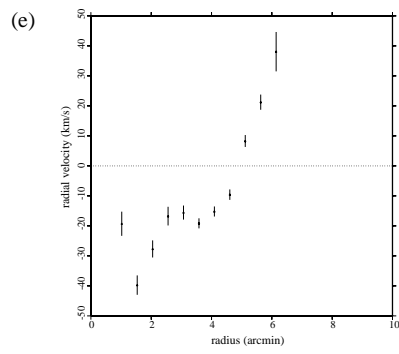
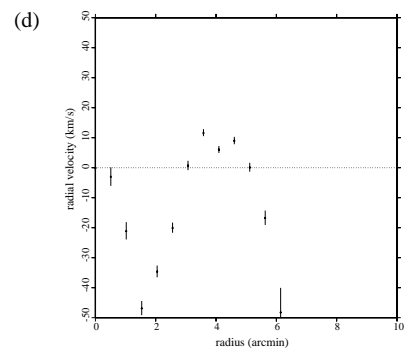
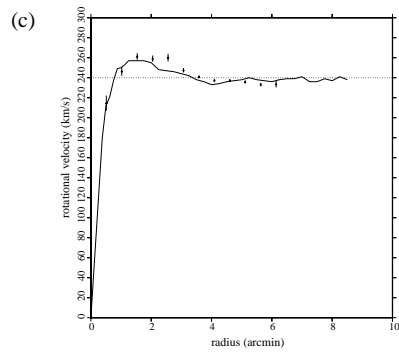
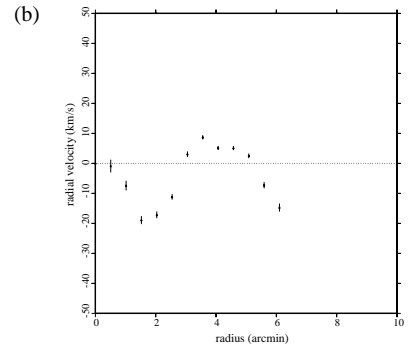
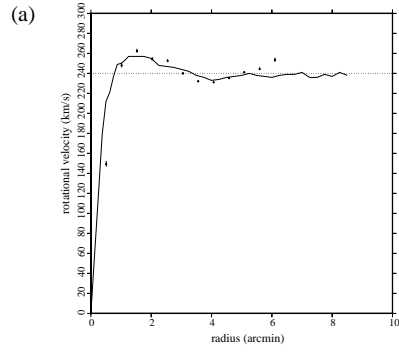


Figure 16: **NGC 7331 Radial Fits.** (a) Two-parameter fit, circular velocity. (b) Two-parameter fit, zeroth-order radial velocity. (c) Four-parameter fit, circular velocity. (d) Four-parameter fit, zeroth-order radial velocity. (e) Four-parameter fit, second-order radial velocity. (f) Four-parameter fit, phase of second-order radial velocity. The solid curve in (a) and (c) is Begeman's, and the horizontal lines are for reference only.



4.6 NGC 2903

NGC 2903 is a type Sc(s)I-II spiral (Sandage and Tammann 1981). It is moderately inclined, and its velocity map (Figure 1f) shows the distinct shift in the contours that is usually taken as a warp signature. Some twists in the southwestern quadrant due to one of the spiral arms ruin what would otherwise be a very clean, bilateral symmetry.

As with NGC 7331, the tilted-rings fits match Begeman’s results quite well. Unlike NGC 7331, the radial extent of the scan-based analysis (out to approximately $10'$) is much closer to Begeman’s ($13'$ for the circular velocity, $12'$ for the inclination and position-angle curves). Figure 17a shows the circular velocities; the only feature of note is the discrepancy between $1.5'$ and $3.5'$, where the current fit is up to 10 km/s (5%) lower than Begeman’s. The result is a rotation curve that is nearly flat, as opposed to Begeman’s, which is somewhat unusual in its steady decline from $2'$ onward.

The inclinations (Figure 17b) also differ slightly from Begeman’s (Figure 17c) at small radii, but the difference is only about 2° (or 2σ of the formal least-squares errors) and vanishes beyond the jump at $6'$. The qualitative “zig-zag” is reproduced well. And the match between the two fits’ position-angle curves is nearly perfect (Figures 17d and 17e).

The radial-oscillations fits also tended to produce flatter rotation curves than Begeman’s (Figures 18a and 18c), but the matches are still good. The radial-velocity curve in the two-parameter fit (Figure 18b) is smooth and reasonable-looking, with an implied infall in the inner region rising to 15 km/s at $6'$, a node at $8'$, and an outflow beyond $8'$ approaching 12 km/s at $10.5'$. The zeroth-order and second-order radial velocities in the four-parameter fit, on the other hand, both have magnitudes as high as 40 km/s at radii as small as $3'$ (Figures 18d and 18e). Once again the fit is balancing large numbers unrealistically. (Note that between $2'$ and $8'$ the phases [Figure 18f] are near 0° , i.e., the galaxy’s major axis, which is

the part of the galaxy where radial velocities cannot be observed; 2'–8' is also the radial region in which the zeroth-order and second-order velocities are largest *and of the same sign*. In other words, the large velocities add where they cannot be observed—along the major axis—and cancel each other along the minor axis where they could be observed.)

So the four-parameter fit is not at all credible, but the two-parameter fit seems reasonable. That reasonableness is significantly diminished when the residuals are considered. Figures 19a and 19b show the residuals maps for the tilted-rings and two-parameter radial fits. The latter map is visibly poorer than the former, with the tilted-rings fit showing distinctly smaller residuals in all areas of the galaxy except along the innermost ring. The “chi-by-eye” effect is borne out by the corresponding RMS residuals: 6.5 km/s and 8.0 km/s for the tilted-rings and two-parameter radial fit, respectively. (The RMS residual for the four-parameter fit was 5.7 km/s.) While both fits are considerably poorer by this metric than were the fits for NGC 3198, NGC 6503 and NGC 2403, it is clear that the tilted-rings model is decidedly superior for NGC 2903.

Figure 17: **NGC 2903 Tilted-Rings Fits.** Our fits are on the left; Begeman's are on the right, except as noted. (a) Circular velocities; the solid rotation curve is Begeman's fit, and the horizontal line is for reference only. (b), (c) Inclinations. (d), (e) Position angles.

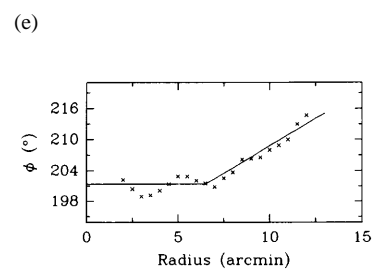
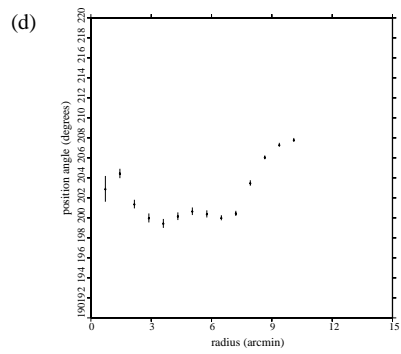
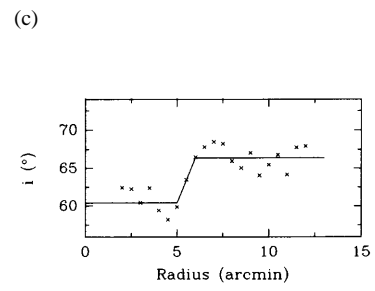
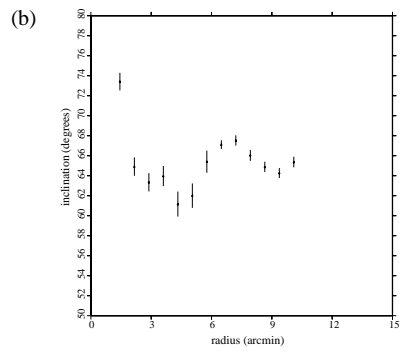
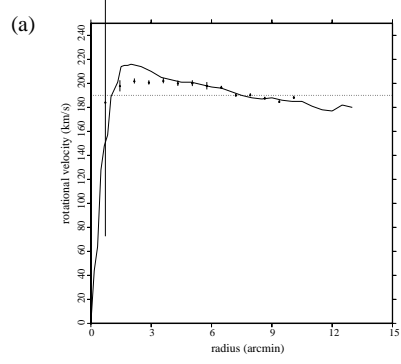


Figure 18: **NGC 2903 Radial Fits.** (a) Two-parameter fit, circular velocity. (b) Two-parameter fit, zeroth-order radial velocity. (c) Four-parameter fit, circular velocity. (d) Four-parameter fit, zeroth-order radial velocity. (e) Four-parameter fit, second-order radial velocity. (f) Four-parameter fit, phase of second-order radial velocity. The solid curve in (a) and (c) is Begeman's, and the horizontal lines are for reference only.

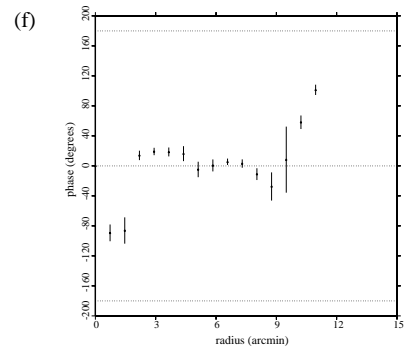
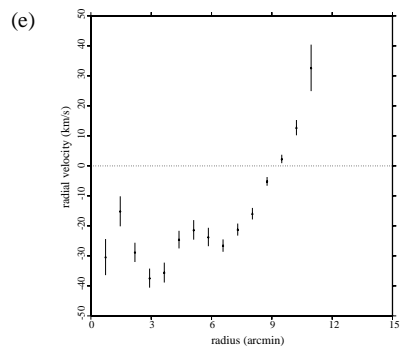
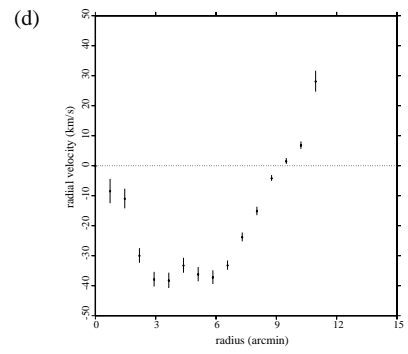
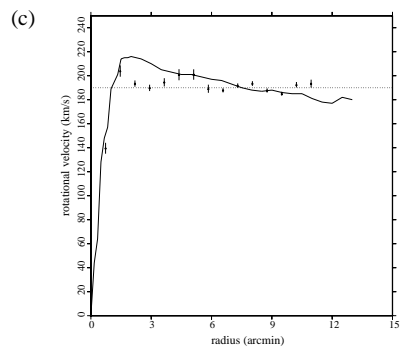
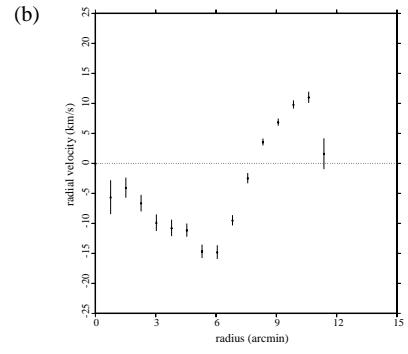
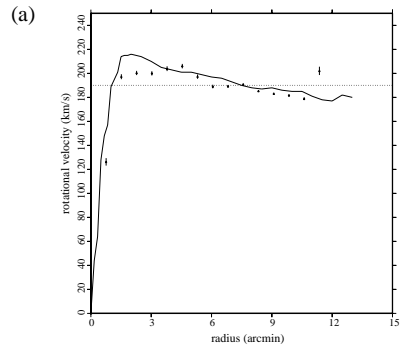
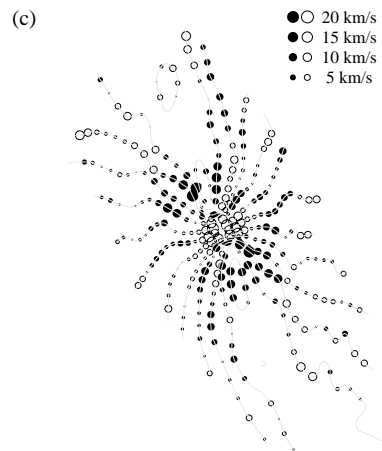
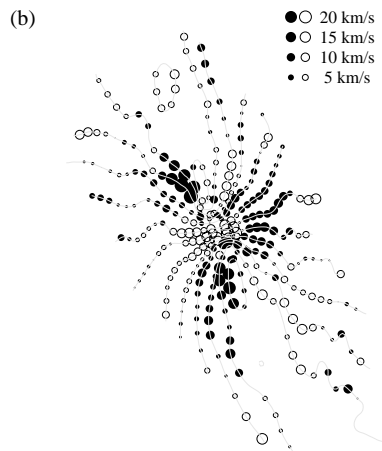
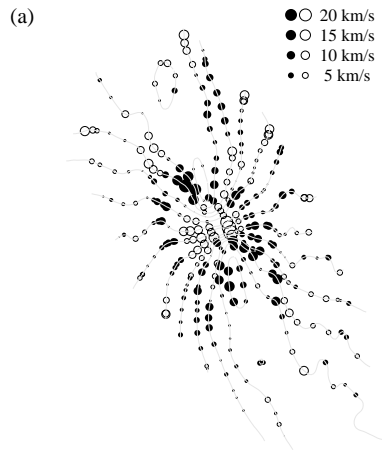


Figure 19: **NGC 2903 Residuals.** (a) Tilted-rings fit; RMS residual is 6.5 km/s. (b) Two-parameter radial fit; RMS residual is 8.0 km/s. (c) Four-parameter radial fit; RMS residual is 5.7 km/s.



4.7 NGC 628

NGC 628 (a.k.a. M74) is a type ScI spiral (Kamphuis and Briggs 1992). It is unusual in this selection of galaxies in that it is almost perfectly face-on. As such its “dipolar” velocity map (Figure 1b) is so exaggeratedly asymmetric as to appear almost symmetric after all. Note that the central pair of contours (650 and 660 km/s) are in fact Z-shaped (with “serifs” on the ends). NGC 628 also stands out by virtue of being rather unambiguously warped and therefore presumably harder to fit with radial flows; it was chosen for this reason.

The unusually low inclination of NGC 628 makes fitting difficult. The circular velocity v_c and inclination i appear in fits to the line-of-sight velocity as the product $v_c \sin i$ and thus cannot be separated within the accuracy of the observations. However, with some reasonable assumptions one may derive good estimates for the model parameters.

Following the method of Kamphuis and Briggs, a two-part tilted-rings fit was performed. In the first part, only the innermost part of the galaxy was fit, $R < 3'$, and the inclination was held fixed at an *assumed* value of 6.5° . From this fit were obtained the global parameters: the sky position (x_0, y_0) of the center of the galaxy and the systemic velocity v_{sys} . These parameters were then held fixed for the second half of the fit, where all of the galaxy data were used. In this part of the fit, the inclination was again held fixed for $R < 3'$ but allowed to vary outside that radius; the circular velocity, on the other hand, was allowed to vary inside $4'$ but was held fixed at 200 km/s for $R > 4'$.

The result of the two-part tilted-rings fit is shown in Figure 20. The derived circular velocity inside $4'$ is slightly higher than the KB result but still within error bars. The inclinations (Figures 20b and 20c) match beautifully, with the sharp dip at $7'$ and final plateau at 14° reproduced perfectly; the only difference is a slightly more rapid rise in the inclination between $7'$ and $10'$, but the choice of ring radii may account for that. The position angles (Figures 20d and 20e) are likewise reproduced

nearly perfectly. Keep in mind also that the data points used in the current scan-based fits are not evenly distributed; unlike higher-inclination contour maps where the contours are U-shaped and tend to lie roughly perpendicular to the rings at the points at which they intersect, the nearly face-on velocity map for NGC 628 has very round, almost circular contours over much of its area. This results in fewer intersections with the rings and is arguably another drawback of the scan-based method, but the excellence of the fit belies that conclusion. The RMS residual, 7.7 km/s, was high due to the irregular outer regions of the galaxy, but the residuals map (Figure 21a) shows that the number was inflated by poor results in only two compact regions on the east and west sides.

The radial-velocity fits are particularly interesting, but not for the same reasons as in any of the previous fits. Rather, the interest stems from the fact that they're so appallingly *bad*. A similar two-part fitting procedure was followed for the radial fits; for the first pass a small-radius subset of the data was used to determine the galaxy's central position and systemic velocity, and these parameters were then held fixed for the second, full-galaxy pass. For the cases where the circular velocity was allowed to vary, it varied wildly (Figures 22a and 22c); to compensate, so did the radial velocities—exceeding 100 km/s at some radii (Figures 22b, 22d and 22e). Holding the circular velocity fixed beyond 4', either at 110 km/s (the initial plateau value) or at 250 km/s (the final plateau value) was even worse: typical radial velocities approached or exceeded 200 km/s, with one hitting 900 km/s. The 250 km/s circular-velocity case is shown in Figure 23. Residuals maps for both types of radial-velocity fits are shown in Figures 21b–21e.

Figure 20: **NGC 628 Tilted-Rings Fits.** Our fits are on the left; Kamphuis and Briggs' are on the right, except as noted. (a) Circular velocities; the solid rotation curve is Kamphuis and Briggs' fit. (b), (c) Inclinations. (d), (e) Position angles. The rotation velocity was held fixed beyond $4'$ and the inclination held fixed for radii smaller than that, as described in the text.

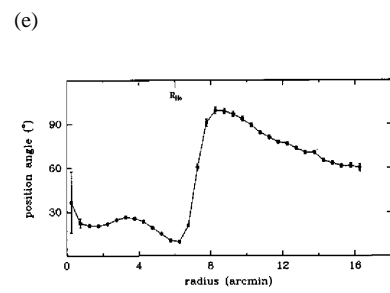
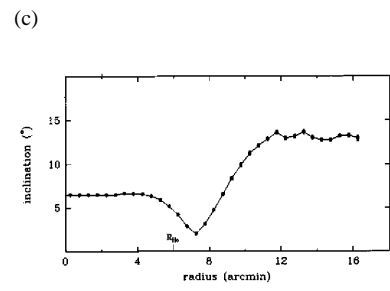
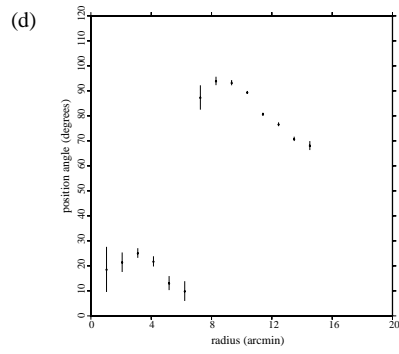
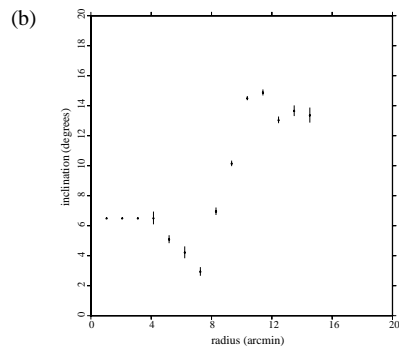
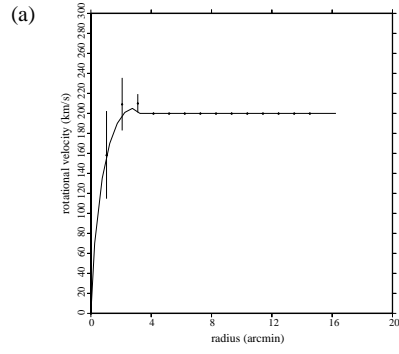


Figure 21: **NGC 628 Residuals.** (a) Tilted-rings fit; RMS residual is 7.7 km/s. (b) Two-parameter radial fit with circular velocity allowed to vary; RMS residual is 7.8 km/s. (c) Four-parameter radial fit with varying circular velocity; RMS residual is 7.3 km/s. (d) Two-parameter radial fit with circular velocity held fixed beyond 4' at 250 km/s; RMS residual is 8.6 km/s. (e) Four-parameter radial fit with fixed circular velocity; RMS residual is 8.8 km/s.

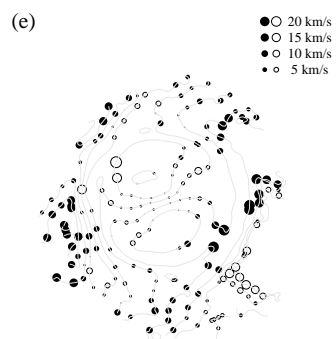
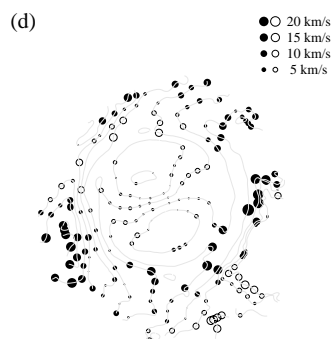
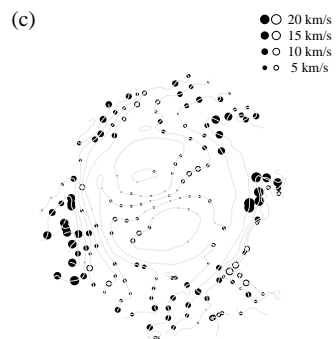
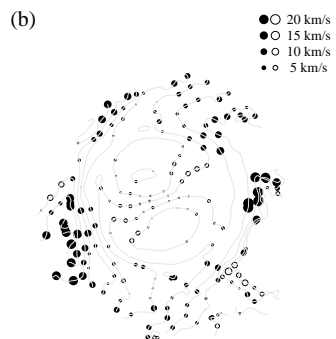
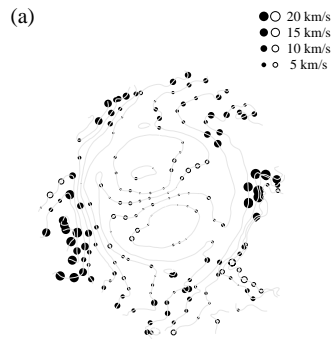


Figure 22: **NGC 628 Radial Fits, Circular Velocity Allowed to Vary.** (a) Two-parameter fit, circular velocity. (b) Two-parameter fit, zeroth-order radial velocity. (c) Four-parameter fit, circular velocity. (d) Four-parameter fit, zeroth-order radial velocity. (e) Four-parameter fit, second-order radial velocity. (f) Four-parameter fit, phase of second-order radial velocity. The solid curve in (a) and (c) is Kamphuis and Briggs', and the horizontal lines are for reference.

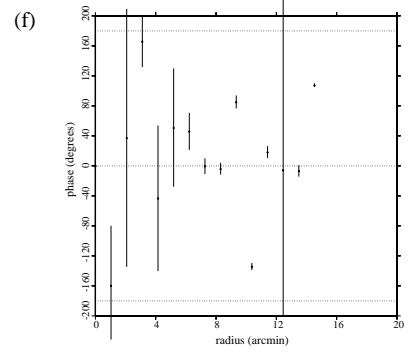
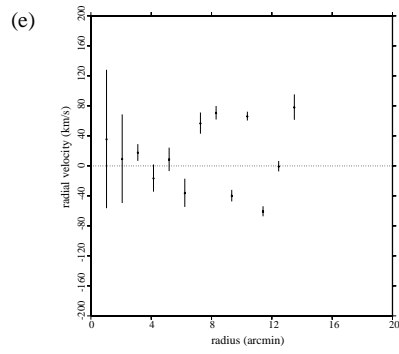
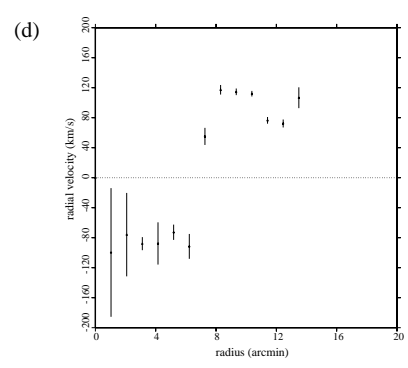
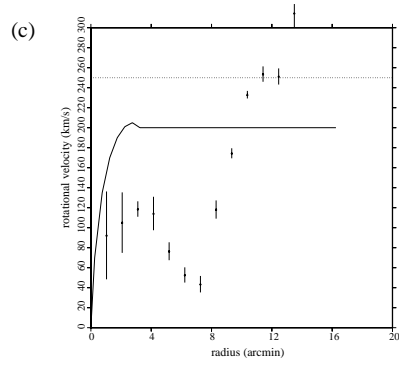
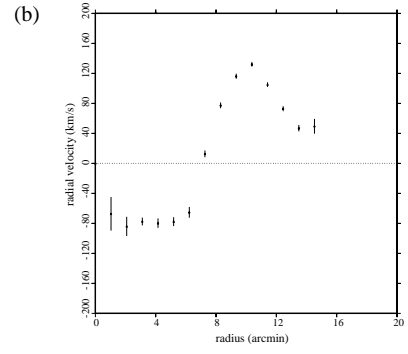
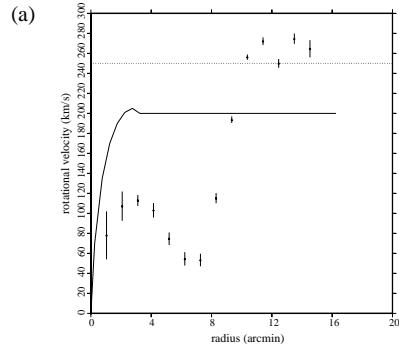
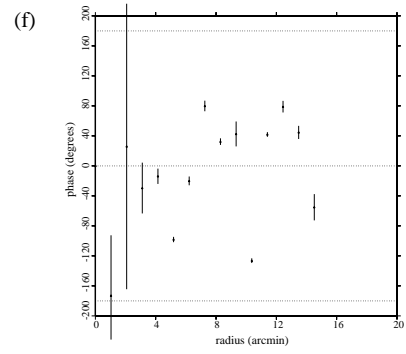
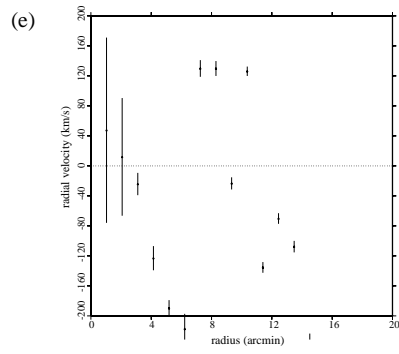
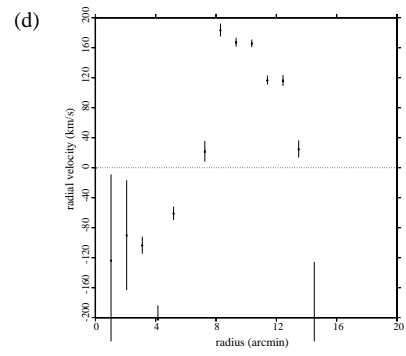
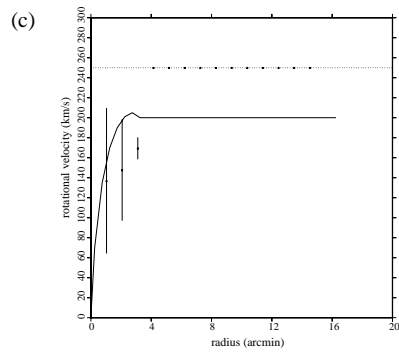
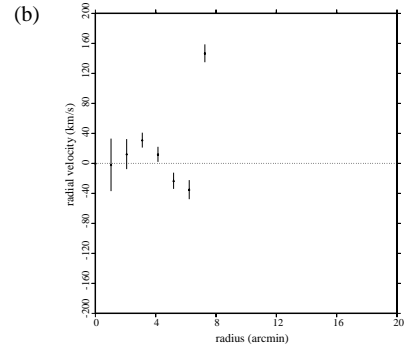
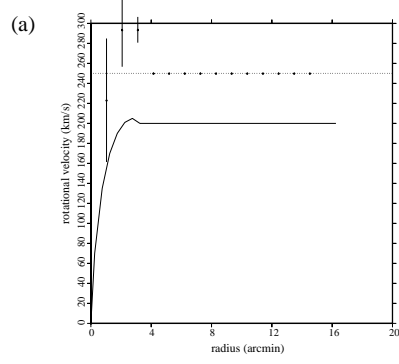


Figure 23: **NGC 628 Radial Fits, Circular Velocity Fixed Beyond 4'.** (a) Two-parameter fit, circular velocity. (b) Two-parameter fit, zeroth-order radial velocity. (c) Four-parameter fit, circular velocity. (d) Four-parameter fit, zeroth-order radial velocity. (e) Four-parameter fit, second-order radial velocity. (f) Four-parameter fit, phase of second-order radial velocity. The solid curve in (a) and (c) is Kamphuis and Briggs', and the horizontal lines are for reference.



CHAPTER 5

DISCUSSION

Bearing in mind the usual caveats about using a one-number metric such as the RMS residual velocity to compare fits, there are a number of observations to be made. First among these is the fact that the four-parameter radial fit basically can be ruled out as not useful. Without exception, the four-parameter fits were either comparable to the two-parameter ones—that is, producing similar, reasonable velocities with only slightly improved residuals—or much worse due to unrealistically large velocities. NGC 3198, NGC 6503 and NGC 2403 fell into the former category; NGC 7331 and NGC 2903 were good examples of the latter. NGC 628 was a little of both: the four-parameter fit was comparable to the two-parameter fit because *both* produced unbelievably immense radial velocities. With higher-resolution data it is conceivable that the four-parameter fit may prove useful, but with the current set it appears that any nominal improvement in the fitting is simply due to having twice as many degrees of freedom per ring.

The two-parameter radial fit looks somewhat more promising, however, despite the fact that none of the galaxies' radial fits showed the unambiguous linear growth that would correspond to the theorized breathing mode. NGC 6503 was close—its curve (Figure 9b) appears to be zero out to $6'$ and then grows linearly (not counting the outermost ring, which can probably be ignored); it is also not too far off from a purely linear curve. With a great deal of imagination NGC 2403 might also be considered vaguely linear (Figure 12b), but the other four galaxies all show one or two nodes. The RMS residuals reflect this to a large extent. For NGC 3198 and NGC 6503 the radial-motions fit performed almost as well as tilted rings; for NGC 2403 the two performed virtually identically. Again, note that the tilted-rings fit has an extra free parameter per ring. Yet while neither type of fit worked

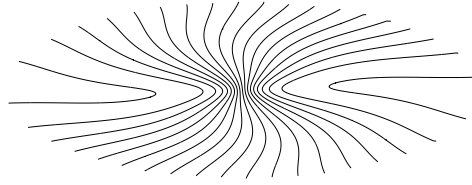
particularly well for NGC 7331 or NGC 2903, in both cases the radial-oscillations fits performed noticeably more poorly—particularly for the latter galaxy. And in the single low-inclination case, NGC 628, the tilted-rings fit was unquestionably better.

This final result suggests a possible observational test for the presence of radial oscillations. Since the two models produce such drastically differing fits in this case, a survey of perhaps a dozen or two low-inclination galaxies should suffice to place some bounds on the presence (or absence) of radial motions. It should be noted that NGC 628 is not necessarily an abnormal example, either, at least with respect to the poorness of the radial fit. It is, in fact, clear from inspection of the velocity map that NGC 628 *cannot* be well-fit by any reasonable two-parameter (azimuthally symmetric) radial model: the “circular arc” portions of the outer contours imply that there is a corresponding distinct change in the rings’ azimuthal orientation (that is, in the position angles). This becomes more intuitively obvious when a radially oscillating fake galaxy is viewed at various inclinations (Figure 24). The maps are qualitatively the same; if the line-of-sight velocity were unaffected by the $\sin i$ inclination factor—that is, if the contour spacing didn’t vary inversely with the inclination due to projection effects—the maps would differ only by a linear scale factor along the minor axis (a “stretching” of the plot vertically in Figure 24). Such stretching does not admit of arclike features such as those seen in the velocity map for NGC 628.

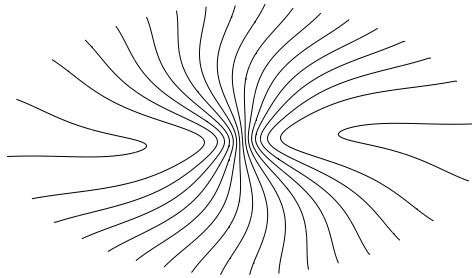
A more direct test for the presence of radial motions is to make high-resolution observations along the minor axis of a relatively highly inclined galaxy. Figures 2b and 2c illustrate the idea. Recall that for this test a fake galaxy was created with radial motions; the corresponding velocity map (Figure 2b) was fed into the tilted-rings program, and the resultant fit produced the velocity field shown in Figure 2c. As noted previously, along the minor axis the two maps differ: the central contour in the original map is integral-shaped, while that from the tilted-rings model is straight.

Figure 24: **Faked Velocity Maps at Various Viewing Angles.** These maps correspond to a radially oscillating, planar galaxy, as described in the text. (a) Inclination 68 degrees (same as Figure 2b); contour separation is 15 km/s. (b) Inclination 55 degrees, contour separation 15 km/s. (c) Inclination 10 degrees, contour separation 5 degrees. Note that all three velocity maps are fundamentally similar; the arc-like features in NGC 628's velocity map (Figure 1b) do not magically appear at low inclinations without a twist in the orientation of the galaxy.

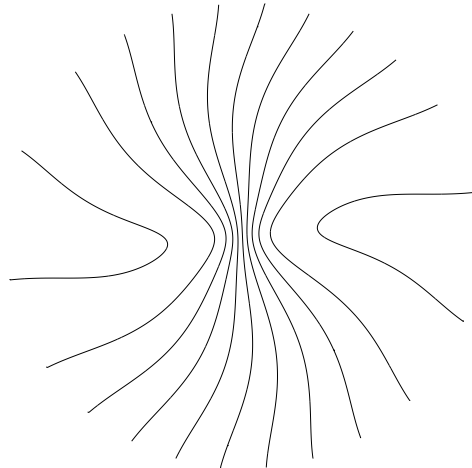
(a)



(b)



(c)



There are, however, several complicating factors with this approach. While the minor axis of any tilted-ring-model ring will show zero line-of-sight velocity—the rotational velocity is strictly perpendicular—there is no guarantee that the minor axis of most of the rings will coincide with the overall minor axis of the galaxy. Any misalignment will produce a small component of the circular velocity along the line of sight, although to judge by Figure 2c, this component may be undetectably small.

More troublesome is the question of spiral arms. Most velocity maps show some hint of the underlying spiral structure; it tends to produce waviness in the contours very much like that seen in velocity map for the faked radial-motions galaxy (Figure 2b). In fact, Canzian (1993) raised the concern that a rings-based model that can change the orientation of every ring—the definition of a tilted-rings model—is likely to be susceptible to “following” the spiral structure, thereby enhancing the presumed warp (or even creating one where none actually exists). Consider NGC 3198, for example, whose arms wrap clockwise; as seen in Figure 7d, the tilted-rings position angle decreases linearly for $R > 2'$, which would correspond to a clockwise spiral. Without taking into account projection effects this is merely suggestive; but in any case, the point is that spiral arms may produce a component of line-of-sight velocity along the minor axis even in the absence of global radial motions. Limiting the high-resolution observations to the minor axes of S0 galaxies would presumably minimize this problem.

Finally, a bar will cause non-circular motions, again allowing a line-of-sight component along the minor axis of a galaxy. There is some evidence that NGC 3198 has a bar, for example; Begeman comments on it. In general bars are restricted to the inner regions of the galaxy, however. The effect on the outer portions of the contours should be minimal.

Besides the relatively direct tests proposed here, it would be convenient if something could be said about the relative probabilities of warps vs. radial motions on the basis of the residuals maps. Figure 4f, the tilted-rings residuals map for the faked, radially oscillating galaxy, suggests the possibilities here; it clearly has

a bilateral mirror symmetry along the major axis, as well as a threefold azimuthal symmetry. Unfortunately a great many such faked fits would be required for even an intuitive heuristic, much less any sort of statistical measure; even a single warp model would need to be viewed at a variety of azimuthal angles. Regardless, the real residuals maps in this paper are considerably less well-behaved. NGC 3198, for example, shows a hint of the threefold symmetry in its tilted-rings fit (Figure 6a); but if anything, that pattern is even more pronounced in the two-parameter radial fit (Figure 6b).

With regard to the efficacy of the scan-based method as an alternative to direct use of the original observational data, the first observation to be made is that it works remarkably well even when the sampling is not uniform, as exemplified by NGC 628. That said, there are unexplained discrepancies in the tilted-rings fits of a couple of the galaxies, notably the shape of the inclinations curve for NGC 3198 (Figures 7b and 7c) and the two-degree offset of the outer inclinations for NGC 2403 (Figures 11b and 11c).

Advantages of the method include the ability to test galaxies where the data are simply not available any other way; the fact that there is no particular need to know the gruesome details of radio-observation data reduction; and the possibility of faster results, depending on the researcher's connections with observers. Drawbacks include the problem of face-on galaxies with arc-like contours (NGC 628); the limited radial extent, most dramatic in the case of NGC 7331, but showing up to some extent in all of the galaxies, especially for the rotation curves; the fact that the data are poorest in the region where the original data were most accurate (along the major axis); the difficulty of estimating errors; and the fact that the method is more time-consuming and labor-intensive than expected.

CHAPTER 6

CONCLUSIONS

To summarize, then, we note the following:

- The derived rotation curves for all of the galaxies except NGC 628 (nearly face-on) are essentially invariant, regardless of model. While this is comforting in the sense that one can trust a given rotation curve to be an accurate reflection of the galaxy's true kinematics, it also means that the curve is useless as a way to distinguish between competing models.
- The four-parameter radial fits are either not much better than the two-parameter radial and (three-parameter) tilted-rings fits, or else they're considerably worse. For this sample of galaxies, at least, they are discounted.
- There is some evidence for radial motions but nothing unambiguous. NGC 6503 and NGC 2403 show the most promise, with radial-velocity curves that at least vaguely resemble the theorized fundamental mode of oscillation (the breathing mode). NGC 3198's radial-velocity curve has two nodes in it, but the fit is otherwise reasonable and competitive with the tilted-rings approach.
- The evidence for warps is excellent in the case of NGC 628 and very good in the cases of NGC 7331 and NGC 2903. (This is not to say that the fits themselves are necessarily good; NGC 7331, for example, clearly has a great deal more going on in it than these simple models can account for.) The tilted-rings model performs roughly equivalently to the radial-motions model in the other three cases, as noted above. That, coupled with the results of the tilted-rings fits, implies that there is good but somewhat ambiguous evidence

for warps in the cases of NGC 3198 and NGC 6503. NGC 2403 does not show evidence of a warp, despite the goodness of the tilted-rings fit.

Taken together, these points are consistent with the idea of all spiral galaxies as potentially warped but not radially oscillating. They are *not* consistent with the idea of all spirals as radially oscillating but not warped; but then, that has been obvious from the beginning: many galaxies are visibly (morphologically) warped. Since the sample is small, one can draw no further conclusions about the presence or absence of radial flows without more direct tests. Fits to nearly face-on galaxies and high-resolution observations of the minor axes of spirals would both be useful to help settle this question.

Simply on the basis of the theoretical predictions, however, it is clear that current tilted-rings fits are incomplete and that, to some extent, they are assuming their conclusion: excluding radial motions from the model ensures that the fits will produce nothing but warped galaxies with no radial velocities. The addition of a single free parameter per ring—the zeroth-order radial velocity—would go far in rectifying this situation. Since the tilted-ring and radial-motions models are not actually mathematically degenerate, such a hybrid fitting program should produce useful results without introducing an unacceptable level of uncertainty into the fitted parameters. Unfortunately, difficulties in writing our own tilted-rings program prevented us from attempting this; the program is currently good enough to allow comparisons both to the radial-motions fit and to previously published tilted-rings results, but it needs more work before it can be considered production code. (Among other things, the current version has some undesirable behavior with respect to rings near the edge of the data, as noted in §4.1.) Extending the fit to include the zeroth-order radial velocity appears to be a straightforward modification, however.

The situation would further improve if galaxies could be “corrected” for spiral structure prior to fitting. That is to say, one would like to be able to remove from the velocity maps those features that are due to the underlying spiral structure; else tilted-rings fits are liable to “absorb” the spiral structure into the warp, as noted

by Canzian (1993). This makes the fitting procedure more complex and may require higher-resolution observations, but the alternative is tilted-rings fits that produce misleading or incorrect warps.

Finally, we note that the scan-based analysis method produces acceptable, useful results. As expected from the outset, however, it is inferior in most respects to the normal analysis method based on original data. Overall, we judge the method useful if and only if there is no alternative.

APPENDIX A

SCAN-BASED DATA ANALYSIS

The sort of image analysis used here begins with a scan of a velocity-field contour map. The resulting bitmap is first edited to remove scanning artifacts and then fed into a tracing program for conversion to a machine-readable format consisting solely of contour data (“vector format”). Finally these contour data are fed into a fitting program.

The scan is straightforward. Experience has shown that the resultant bitmap should measure at least 1000 pixels linearly, and in practice images greater than 2000×2000 are unnecessarily large. This means that, with a 400 dot-per-inch scanner, a three-inch (7.6 cm) contour map will suffice—a small enough image size to include most published maps—and anything larger than $4'' \times 6''$ (10cm \times 15cm) can be subsampled as desired.

Editing the bitmap is easily the most tedious part of the process. In addition to removing intentional and accidental artifacts such as labels, fiducial marks, dust specks and so forth, it is also generally necessary to “split” the image into two, three or four interleaved parts by erasing all but every n th contour (“decimation,” loosely speaking). This is due to limitations of the tracing program; it is not smart enough to avoid “jumping the tracks” in regions where the velocity gradient is steep—i.e., where the contours bunch together and may even touch due to lack of precision in plotting, reproduction and/or scanning. The simplest way to avoid this problem is to remove the neighboring contours.

The conversion of the (raster) bitmap image into a linear (vector) representation of each of the contours is more automated but still requires enough human input to be somewhat tedious as well. The tracing program begins with a user-provided pair of coordinates that defines a contour-crossing line segment; the

program traverses this line looking for intersections with contours. It then loops over the intersections and traces each contour to its endpoint (or, in the case of closed contours, until it hits a previously marked point) without writing anything. Finally it reverses direction and (re)traces the entire contour, writing the data in the form of very short line segments (typically ten pixels in length). None of this is particularly difficult; the problems arise when there are cusps (causing the program to stop tracing prematurely) and outlying closed contours not crossed by the original line segment, which must be dealt with separately. Even in the case of a nearly ideal galaxy, there is no automatic way to assign velocities to the traces and reassemble them in order, and the program often traces closed contours several times before hitting a previously marked dot and terminating.

Since perfect alignment of the the velocity map with the scanner is highly improbable, the scanned data must be corrected for the relative rotation between the two. Failure to do so shows up as a constant shift in the position angles. There is also a small amount of distortion in the scan. Both effects are cancelled quite nicely by means of a linear transformation, and the calibration between scan units and actual sky coordinates (right ascension and declination) is a convenient side-effect. This is accomplished by means of two pairs of approximately parallel lines joining appropriate tick-marks on the axes of the scanned map; the four lines intersect at four points approximating a rectangle, as in a tic-tac-toe board. At each of the four points, the (x, y) coordinates are known in both scan units and sky units, and this suffices to find the appropriate transformation between the two coordinate systems.

In fitting it is necessary to associate velocity-position data with the model's ring structure. The general case of assigning to an arbitrary location a velocity based on the values of the nearby contours is extremely difficult; this would require two-dimensional, irregular interpolation, something for which there seems to be no well-established procedure. The approach taken here is much simpler and, in some sense, more precise: rather than following each ring and interpolating velocities at arbitrary points, we follow the contours and calculate the points on each one

where a given ring intersects it. This amounts to calculating the radius of each contour point in the plane of the galaxy (or of the ring, in the tilted-rings fit) and linearly interpolating between the pairs of contour points that encompass each ring intersection. The intersection points are sorted according to the rings on which they lie, and rings with too few data points are discarded from the fit.

Error estimation in the scan-based method is something of a black art. The scan itself introduces a small amount of distortion, as noted above, but the calibration step corrects for that. There is also presumably some error in the printed map itself—we are not counting the original, observational errors in the data but rather those introduced by the contouring routine and by the publishing process. There is no good way to get a handle on these errors; we chose an ad hoc value of 2 km/s, which is probably a bit generous. Finally, the contour-tracing step is likely to be the principal source of systematic errors. Since each scanned contour is typically 6–12 pixels wide, we can assume the tracing error amounts to a fixed number of pixels. The exception is in those regions where the contours approach each other more closely than the printed line width and therefore touch; the error is slightly bigger there. Conversion from pixels to kilometers per second depends on the velocity gradient: low in the outer regions and quite high near the center. We assign tracing errors on a per-ring basis, depending on the radius (in pixels). This is not particularly precise (the contour spacing varies somewhat over each ring), but the idea is simply to get an approximate idea of how trustworthy the fits are. These estimates suffice for that purpose.

REFERENCES

- Arp, H. C., and Kormendy, J., 1972. *Astrophys. J. Lett.*, **178**, L101.
- Begeman, K., 1987. Ph.D. thesis, University of Groningen.
- Begeman, K., 1989. *Astron. Astrophys.*, **223**, 47.
- Binney, J., 1990. In *Dynamics and Interactions of Galaxies*, ed. R. Wielen (Berlin: Springer-Verlag), 328.
- Binney, J., 1992. *Annu. Rev. Astron. Astrophys.*, **30**, 51.
- Bosma, A., 1981. *Astron. J.*, **86**, 1791.
- Bosma, A., 1991. In *Dynamics of Disk Galaxies*, ed. B. Sundelius (Göteborg, Sweden: Göteborg University Press), 71.
- Briggs, F. H., 1990. *Astrophys. J.*, **352**, 15.
- Brinks, E., and Burton, W. B., 1984. *Astron. Astrophys.*, **141**, 195.
- Canzian, B., 1993. *Astrophys. J.*, **414**, 487.
- Christodoulou, D., Tohline, J., and Steiman-Cameron, Y. C., 1993. *Astrophys. J.*, **416**, 74.
- Kamphuis, J., and Briggs, F., 1992. *Astron. Astrophys.*, **253**, 335.
- Lynden-Bell, D., 1967. *MNRAS*, **136**, 101.
- Miller, R. H., and Smith, B. F., 1994. *Celestial Mechanics and Dynamical Astronomy*, **59**, 161.
- Press, W. H., Teukolsky, S. A., Vetterling, W. T., and Flannery, B. P., 1992. *Numerical Recipes in C: The Art of Scientific Computing*, second ed. (New York: Cambridge University Press), 683.

- Rubin, V. C., Ford, Jr., W. K., and Peterson, C. J., 1975. *Astrophys. J.*, **199**, 39.
- Rubin, V. C., Thonnard, N., and Ford, Jr., W. K., 1975. *Astrophys. J.*, **199**, 31.
- Rubin, V. C., Thonnard, N., and Ford, Jr., W. K., 1977. *Astrophys. J. Lett.*, **217**, L1.
- Sandage, A. and Tammann, G. A., 1981. *Revised Shapley-Ames Catalogue of Bright Galaxies* (Carnegie Inst. of Washington Pub. No. 635).
- Shostak, G. S., 1993. Private communication.
- Sparke, L. S., and Casertano, S., 1988. *MNRAS*, **234**, 873.
- Steiman-Cameron, T. Y., and Durisen, R. H., 1988. *Astrophys. J.*, **325**, 26.
- Steiman-Cameron, T. Y., and Durisen, R. H., 1990. *Astrophys. J.*, **357**, 62.
- van Albada, T. S., Bahcall, J. N., Begeman, K., and Sancisi, R., 1985. *Astrophys. J.*, **295**, 305.